npj | microgravity

Article

Published in cooperation with the Biodesign Institute at Arizona State University, with the support of NASA

https://doi.org/10.1038/s41526-024-00429-w

Using noninvasive imaging to assess manual lymphatic drainage on lymphatic/venous responses in a spaceflight analog

Check for updates

Heather Barnhart[1], Frank Aviles Jr[2], Johanna Pannunzio[1], Nathan Sirkis[1], Chantel Hubbard[1], Patrick Hardigan[3], Sabrina Ginsburg[4], Harvey Mayrovitz[5], Kristen A. Eckert[6] & M. Mark Melin[7]

This retrospective case series (clinicaltrials.gov NCT06405282) used noninvasive imaging devices (NIID) to assess the effect of manual lymphatic drainage (MLD) on dermal/venous fluid distribution, perfusion, and temperature alterations of the head, neck, upper torso, and legs while in the 6-degree head-down tilt validated spaceflight analog. A lymphatic fluid scanner measured tissue dielectric constant levels. Near-infrared spectroscopy assessed perfusion, by measuring tissue oxygenation saturation. Long-wave infrared thermography measured tissue temperature gradients. Fifteen healthy, university students participated. NIID assessments were taken 1 minute after assuming the HDT position and then every 30 minutes, with MLD administered from 180 to 195 minutes. Subjects returned to the sitting position and were assessed at post-225 min NIID demonstrated significant changes from baseline ($p < 0.01$), although these changes at areas of interest varied. MLD had a reverse effect on all variables. NIID assessment supported the potential use of MLD to mitigate fluid shifts during a spaceflight analog.

Under the influence of standard developmental physiology on the Earth's surface (1 gravity equivalent, known as "1 g"), 70% of body fluids reside below the level of the heart (Fig. 1)[1]. The lymphatic system has the capacity and capability to transport fluid from distal to proximal in an upward manner, against gravity and tissue pressure gradients, via lymphangion contractility, leg muscle contraction, and respiratory and chest wall function, thus augmenting a "suction effect" for pumping lymphatic fluid within the subatmospheric pressure tissue distribution zones (the Guyton principle)[2]. Lymphatic drainage of the head and neck must be assisted by gravity, since these regions are above the level of the heart. In the weightlessness of space and resulting significant alterations of terrestrial 1 g head-to-foot hydrostatic pressure gradients, astronauts experience a dramatic fluid redistribution of ~2 liters from the legs to the upper torso, head, and neck within the first 24–48 hours of flight, among other cardiovascular and physiologic system adaptations[3–6]. The majority of this fluid redistribution has been shown to occur during the first 6–10 hours of spaceflight, with significant changes possibly occurring as soon as 4 hours postflight[7]. Fluid shifts may result in headaches, congestion, or facial edema that can contribute to deteriorating sleep patterns[4]. Fluid shifts towards the cephalic region during microgravity have been speculated to contribute to the development of spaceflight-associated neuro-ocular syndrome (SANS)[8]. SANS is a distinct, microgravity-induced phenomenon of neuro-ophthalmic findings observed in astronauts following long-duration spaceflight including choroidal folds, optic disc edema, posterior globe flattening, refractive shift, and cerebral fluid shifts noted to be persistent at 6-month postflight MRI scans. Although a significant barrier to spaceflight, the underlying mechanisms of SANS are proposed to be a "multi-hit" sequala[9]. Given the limited medical capabilities in the spaceflight environment, there exists a distinct inability to perform invasive diagnostic testing[8]. Thus, noninvasive approaches to studying real-time fluid shifts in weightlessness could serve as critical areas of research to further SANS study and effective countermeasure protocol development.

Lymphatic research in low earth orbit (LEO) is largely still in a pre-clinical, experimental phase. Murine models involving tail elevation and hindlimb unloading (simulated weightlessness), unmanned space shuttles, and satellites have shown cephalic fluid shifts similar to those reported in astronauts during spaceflight and have demonstrated the redistribution of lymphocytes among organs that decreased their immunologic

[1]Department of Physical Therapy, Dr. Pallavi Patel College of Health Care Science, Nova Southeastern University, Fort Lauderdale, FL, USA. [2]Hyperbaric Physicians of Georgia, Cumming, GA, USA. [3]Research Department; Dr. Kiran C Patel College of Allopathic Medicine, Nova Southeastern University, Fort Lauderdale, FL, USA. [4]Leonard M. Miller School of Medicine, University of Miami, Miami, FL, USA. [5]Department of Medical Education, Dr. Kiran C Patel College of Allopathic Medicine, Nova Southeastern University, Fort Lauderdale, FL, USA. [6]Strategic Solutions, Inc., Bozeman, MT, USA. [7]Gonda Vascular Center, Wound Clinic, Mayo Clinic, Rochester, MN, USA. e-mail: melin.matthew@mayo.edu

response[3,10–16]. To our knowledge, potential, restorative countermeasures to improve lymphangion contractility and overall lymphatic function during spaceflight have not been investigated. In normal gravity environments, MLD is a widely used therapy involving a specialized protocol of gentle, therapeutic massage that reduces lymphatic fluid in areas affected by edema[17–19]. A systematic review and meta-analysis of randomized controlled trials have demonstrated that MLD significantly improves lymphedema symptoms and pain in patients with breast cancer ($p = 0.02$)[19]. The potential use of MLD in microgravity environments to mitigate fluid shifts has not been studied.

The ability to manage, mitigate, or offset fluid shifts is vital to maintain nominal health for short and long-duration spaceflight and potentially improve readaptation to terrestrial gravity or other surface gravity fields, such as the moon or Mars. During deep space missions, ground-based medical teams will no longer be easily accessible due to distance and communication delays, hence crew members must perform point-of-care (POC) functions independently to maintain preventative health measures, along with urgent corrective and potentially curative countermeasures[5]. NIID is now available at POC, which could overcome the previous barriers to continuous fluid shift monitoring during spaceflight. Lymphatic fluid scanners measure the tissue dielectric constant (TDC) in areas of interest (AOI) to determine fluid flow patterns and alterations related to positioning[20,21]. Near-infrared spectroscopy (NIRS) measures oxygenated and deoxygenated hemoglobin to determine superficial tissue oxygenation levels for the monitoring of perfusion changes[22–24]. Increased cerebral oxygenation has been documented as soon as 1.5–3 hours in multiple NIRS studies using the 6-degree HDT model[22,25,26]. In parabolic flight, NIRS has demonstrated that arterial blood flow to the head increased, with cerebral oxyhemoglobin 3 times higher than baseline values[27]. Long-wave infrared thermography (LWIT) provides reliable and reproducible temperature assessments, by measuring physiological tissue temperature differentiation to understand thermal energy emitted from AOI[28–30].

Before evaluating NIID during spaceflight missions, it is important that this technology is first quantified and validated through ground-based analogs[6,31,32]. Ground-based analogs for simulation of the impact of weightlessness on human physiology exist in several forms, including strict 6-degree head-down tilt (HDT) bed rest, dry immersion, and brief periods (20–40 seconds) of weightlessness during parabolic flights[6,7,31–33]. HDT is the most widely used and validated spaceflight analog that addresses fluid shifts in a timely manner[6,31,32].

The main objectives of this pilot, retrospective case series were twofold: (1) to use 3 POC NIID to assess dermal/venous fluid flow patterns, perfusion changes, and temperature differential alterations of the head, neck, upper torso, and legs while in the 6-degree HDT validated spaceflight analog position; and (2) to analyze the effect of MLD therapy administered in the HDT position on the aforementioned variables. We hypothesized that dermal venous and lymphatic flow patterns of the head, neck, upper torso, and ventromedial bundle flow patterns should have shifted to cephalad (indicating dermal interstitial fluid increase) in the 6-degree HDT position and should have been reversed following MLD administered in the HDT position. Tissue oxygenation levels at the affected AOI should have subsequently decreased, while MLD should have reversed those trends. Lymph flow has been shown to appear to be influenced by local tissue temperature in rats[34,35]; MLD should have impacted superficial venous flow (that could have impacted temperature gradients[36,37]) and should have reversed alterations initially observed in the HDT spaceflight analog.

Results

Baseline characteristics

The median (IQR) age of the 15 subjects was 24 years (22–30), and 11 (73%) were female. Table 1 summarizes baseline patient characteristics. All 15 participants underwent imaging with all 3 devices while in the HDT position, but 3 participants unexpectedly had some or all LWIT data missing, because an earlier version of the device was not able to manage the high-volume images taken. It was impossible to externally upload images to save them, but this issue was corrected with the use of a newer device model in the remaining participants.

TDC analysis

Table 2 summarizes the TDC data measured by the lymphatic fluid scanner device and corresponding statistical analysis. Table 2 and Figs. 2–5 demonstrate that, while in the HDT position, TDC levels were generally stable from 30 minutes after assuming position until post-180 min for all AOI, except for the right subclavicular region, where at post-150 min, the median (interquartile range [IQR]) TDC had a noticeable increase from 44.1 (39.7–47.2) at baseline to 44.2 (40.9–47.8), and the marginal mean (standard error [SE]) TDC increased from 44.2 (1.1) to 44.3 (1.6). The mean percent changes from baseline for all timepoints and all AOI always had p values less than 0.10 (Table 2). However, not all differences were statistically significant, because there was a large SE due to the limited sample size, and the 90% CIs crossed the zero-line and, therefore, did not reject the null hypothesis. This is the case for all percent differences at post-180 min, which all have p values less than 0.10 (Table 2), the largest SEs observed, and 90% confidence intervals (CIs) including zeros, rendering the percent differences not statistically significant (Table 2 and Figs. 2–5). Similarly, the increased TDC observed in the right subclavicular region at post-150 min was not significant. Nonetheless, the medians and marginal means at post-180 min all showed a noticeable decrease, which appeared to resolve following 15 minutes of MLD at post-195 min, with median TDC levels greater than or equal to baseline levels for all AOI, except for the right temple and the left ventromedial bundle. Both these AOI had median TDCs greater than baseline at post-225 min in the sitting position. Marginal means for all AOI were greater than baseline at post-195 min (post-MLD).

The temples did not have any significant within-group changes in TDC levels (Table 2 and Fig. 2). TDC levels of the sternocleidomastoid (SCM) were significantly greater than baseline at post-30 min on the right side ($p < 0.10$), and after 30 minutes on the left side; post-60 min on both sides, post-90 min and post-120 min on the left side, and post-150 min on both sides ($p < 0.05$) (Table 2 and Fig. 3). There was a significant increase at post-195 min (post-MLD) on both sides, and post-225 min on the right side ($p < 0.05$). At the right subclavicular region (Table 2 and Fig. 4B), the marginal mean at post-195 min (post-MLD) had a significant different increase of 1.58% (90% CI: 0.71–2.54; $p = 0.003$). At the right ventromedial bundle (Table 2 and Fig. 5B) at post-225 min, the right side demonstrated a significant increase of 1.02% (90% CI: 0.04–2.00; $p = 0.089$).

Tissue oxygenation saturation analysis

Tables 3 and 4 summarizes tissue oxygenation saturation statistical analysis over the course of the study. At the medial knee, proximal leg, and frontal subclavian region, significant decreases on both sides occurred at the post-30 min, post-60 min ($p < 0.05$), post-90 min ($p < 0.001$), post-120 min, post-150 min, post-180 min, and post-195 min ($p < 0.10$) (Table 3). In Table 4, all timepoints demonstrated significant changes at the temporal lobe, venous angle, and forehead ($p < 0.10$), except for post-225 min at the front venous angle and right lateral venous angle.

The median tissue oxygenation levels are plotted in Fig. 6. In Fig. 6A, all left AOI had fluctuations in median tissue oxygenation levels, but these changes were particularly noticeable at the frontal subclavian and frontal venous angle regions, the former of which saw a sharp decrease after the post-150 min timepoint, and the latter of which saw a sharp decrease after 120 minutes. These 2 AOI had equivalent median baseline values, and MLD appeared to result in a sharp increase, with values returning to baseline levels at post-225 min in the sitting position. Right AOI also demonstrated fluctuating tissue oxygenation levels (Fig. 6B), with the largest decrease observed at post-180 min and a small increase observed after MLD at post-195 min for all AOI, except for the lateral venous angle. Figure 7 provides a visual case example of NIRS assessment of the head (face) and neck in a healthy, 28-year-old female subject at key timepoints. A visible reduction of tissue oxygenation levels proportional to the amount of time spent in HDT position is observed. Interestingly, the tissue oxygenation visual levels of the

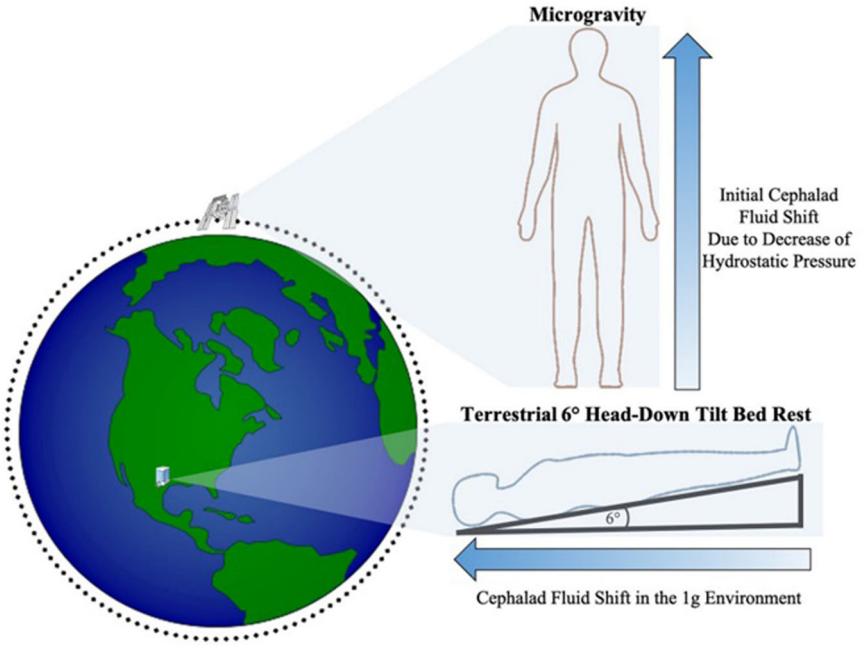

Fig. 1 | Body fluids at 1 g on Earth in spaceflight analog head-down tilt bed rest compared to the weightlessness environment on the International Space Station. This image was previously published by Ong, Lee, and Moss in *Frontiers in Neurology*[1].

neck appeared to increase over time (turning darker red) while in the HDT position, until after MLD (at both post-195 min in the HDT position and post-225 min in the sitting position), when levels turned yellow and even green, signifying they decreased in intensity.

LWIT tissue temperature gradient analysis

Table 5 summarizes the temperature gradient statistical analysis. The right side of the head/neck region and the right leg had abnormal thermal gradients outside the ±1 °C range for most of the timepoints. Generally, the left AOIs remained within the normal thermal gradient, even with significant changes from baseline. For the head/neck region, significant within-group decreases from baseline occurred on the left and right side at post-60 min and post-90 min ($p < 0.05$), on all sides at post-120 min, on the front and left side at post-150 min and post-180 min ($p < 0.10$), at the left side at post-195 min ($p = 0.047$), and on the front at post-225 min ($p = 0.019$). On the legs, the right side had a significant decrease at post-60 min ($p = 0.081$), and both sides had a significant decrease at every point thereafter ($p < 0.05$).

Figure 8 and Table 5 show the median tissue temperature gradient levels over the course of the study. Generally, the legs showed a decreasing trend in temperature gradient even after MLD, while the head/neck AOI fluctuated more (particularly for the front and left side), but a noticeable increase was shown after MLD at post-195 min for the front and left head/neck. The right head/neck was more constant throughout the study. Figure 9 depicts a case example of LWIT image taken from the same subject represented in Fig. 7. An initial increase in temperature gradient at the head and neck was greater on the right side, compared to the left, indicating suspected venous engorgement over time in the HDT position. After MLD at post-195 min in the HDT position and post-225 min in the sitting position, there was a visual reduction of perfusion (or venous engorgement) in the head and neck towards normalcy.

Table 1 | Patient baseline characteristics ($n = 15$)

Variables	Median no. of subjects (IQR)
Age, years	24 (22–30)
Race/ethnicity	
White	9 (60)
Hispanic	2 (13)
African American	2 (13)
South Asian/Indian	1 (6)
Asian	1 (6)
Sex	
Male	4 (27)
Female	11 (73)
Heart rate	71.0 (64.0–77.0)
Systolic blood pressure	119.0 (113.0–124.0)
Diastolic blood pressure	71.0 (69.0–77.0)
Respiratory rate	20.0 (18.0–22.0)
Body temperature, °C	36.7 (36.6–36.8)
Blood oxygenation, %	98.0 (96.0–99.0)

Continuous variables are summarized as medians [interquartile ranges (IQR)]. Categorical variables are summarized as counts (percentages).

Vitals analysis

Table 6 summarizes vitals data. All vitals were normal at baseline. Blood oxygen levels remained stable throughout the course of the study. A significant within-group change from baseline occurred at all timepoints for heart rate. Median heart rate values decreased over the first 180 minutes, while marginal means fluctuated with all timepoints demonstrating significant change; the largest change from baseline was a decrease by 7.90 after 180 minutes. MLD appeared to then increase heart rate from a median (IQR) of 58.5 (54.0–71.0) and a marginal mean (SE) of 62.6 (2.5) at post-180 min to 67.0 (60.0–77.0) and 66.7 (2.5), respectively, at post-195 min Systolic blood pressure remained stable in the HDT position and then significantly increased by 6.60% (90% CI: 2.52 to 10.68, $p = 0.008$) when put in the sitting position for the final 30 minutes. Diastolic blood pressure generally increased from baseline, with significant changes observed from post-90 min thereafter ($p < 0.1$) and with the largest increase from baseline observed following MLD at post-195 min [from a marginal mean (SE) of 71.9 (1.4) to 81.4 (1.4), or a 9.47% increase (90% CI: 6.33–12.60, $p < 0.001$)]. The respiratory rate

Table 2 | Summary analysis of tissue dielectric constant measurements captured by lymphatic fluid scanning device (*n* = 15)

Timepoint	Temple		Sternocleidomastoid		Subclavicular		Ventromedial bundle	
	Left	Right	Left	Right	Left	Right	Left	Right
Baseline								
Median	48.3	48.3	49.4	49.0	41.6	44.1	39.7	38.5
Interquartile range	42.1–51.8	40.6–51.9	45.2–53.4	45–52.6	41–47.2	39.7–47.2	36–41.2	36.6–40.4
Marginal mean (SE)	47.6 (2)	47.5 (2)	49.8 (1.5)	49.8 (1.1)	44.4 (1.1)	44.2 (1.1)	40.1 (1.2)	39.6 (0.9)
Post-30 min								
Median	44.1	43.9	50.5	50.1	43.9	44.0	39.8	37.2
Interquartile range	40.8–50.9	40.3–53.2	48.7–54.0	46.7–53.8	40.9–46	40–49.8	36.0–40.9	37.0–40.2
Marginal mean (SE)	46.6 (1.6)	46.2 (2.6)	52 (1.4)	50.8 (1)	44 (1.4)	43.7 (1.2)	40.3 (0.8)	39.5 (0.8)
Mean % change from baseline	0.98	−1.25	2.19	0.97	−0.38	−0.51	0.18	−0.20
90% Confidence Interval	−2.81–0.84	−3.59–1.09	0.97–3.40	0.09–1.86	−2.92–2.17	−2.11–1.08	−0.67–1.03	−0.74–0.35
P value	0.376	0.379	0.003	0.071	0.807	0.597	0.729	0.555
Post-60 min								
Median	46.6	47.0	50.0	49.7	44.1	44.7	40.4	38.5
Interquartile range	44.0–50.2	42.1–50.9	49.2–53.7	46.4–54.1	41.3–46.3	42–46.2	36.6–41	36.4–40.4
Marginal mean (SE)	48.1 (1.4)	48.6 (1.6)	52 (1.2)	51.3 (1.2)	45.2 (1)	45.2 (0.9)	40.1 (0.8)	39.2 (0.8)
Mean % change from baseline	0.48	1.08	2.25	1.51	0.80	1.03	0.01	−0.43
90% Confidence Interval	−1.64–2.60	−0.68–2.85	1.07–3.44	0.90–2.12	−0.44–2.04	−0.35–2.41	−1.26–1.29	−1.46–0.59
P value	0.712	0.313	0.002	0.001	0.289	0.218	0.987	0.488
Post-90 min								
Median	48.6	45.6	50.3	49.7	43.9	44.3	39.5	39.7
Interquartile range	44.2–52.8	43.2–51.5	49–53.7	48.8–53.3	41.6–47.9	42.0–46.2	37.0–40.2	36.3–40.2
Marginal mean (SE)	48.9 (1.6)	47.9 (1.8)	51.9 (1.1)	51.5 (0.9)	46 (1.1)	45.5 (1)	40 (0.6)	39.9 (1)
Mean % change from baseline	1.28	0.47	2.14	1.68	1.64	1.27	−0.15	0.26
90% confidence interval	−0.51–3.08	−1.59–2.53	0.54–3.74	0.55–2.82	0.26–3.03	−0.27–2.82	−1.77–1.47	−0.77–1.28
P value	0.239	0.708	0.028	0.015	0.051	0.175	0.879	0.680
Post-120 min								
Median	46.2	46.0	49.4	49.3	44.0	42.1	39.6	36.9
Interquartile range	44–49.3	43.7–51.4	46.1–55.1	45.2–54.1	40.8–46.2	40.2–44.2	37.5–40.2	36–40.4
Marginal mean (SE)	48.3 (1.2)	47.6 (1.9)	52 (1.4)	50.7 (1.6)	44.8 (1)	36.6 (6.2)	39.8 (0.9)	39.6 (0.9)
Mean % change from baseline	0.64	0.12	2.24	0.9	0.44	−7.62	−0.34	−0.07
90% confidence interval	−1.27–2.55	−2.28–2.53	0.76–3.71	0.58–2.42	−1.13–2.01	−17.23–2.00	−2.27–1.59	−1.02–0.88
P value	0.582	0.933	0.013	0.312	0.647	0.193	0.771	0.905
Post-150 min								
Median	46.0	49.1	50.8	50.9	44.0	44.2	39.3	37.5
Interquartile range	44.1–52.4	44.2–54.2	47–54	45.8–54.2	42.7–46.2	40.9–47.8	36.7–40.3	36.6–40.3
Marginal mean (SE)	48.9 (1.6)	50.3 (1.5)	52.3 (1.5)	51.6 (1.4)	45 (0.9)	44.3 (1.6)	39.8 (0.7)	39.8 (0.8)
Mean % change from baseline	1.26	2.84	2.49	1.82	0.65	0.06	−0.34	0.11
90% confidence interval	−0.85–3.37	1.02–4.67	0.70–4.29	0.40–3.25	−0.71–2.02	−1.96–2.07	−1.42–0.73	−0.87–1.08
P value	0.327	0.010	0.022	0.036	0.431	0.961	0.597	0.859
Post-180 min								
Median	46.1	48.5	49.9	52.9	43.9	44.0	37.6	36.1
Interquartile range	42.8–51.4	43.2–51.2	46–53.7	45.6–54.2	43.2–45.3	41.1–45.2	35.8–40.2	35.0–39.9
Marginal mean (SE)	41.2 (7)	41.6 (7.2)	43.9 (7.4)	45 (7.5)	38.5 (6.6)	37 (6.4)	33.2 (5.9)	32.3 (5.7)
Mean % change from baseline	−6.47	−5.89	−5.86	−4.73	−5.90	−7.18	−6.91	−7.32
90% confidence interval	−17.75–4.81	−16.93–5.15	−17.41–5.69	−16.59–7.14	−16.82–5.03	−17.45–3.09	−16.95–3.13	−17.06–2.42
P value	0.345	0.380	0.404	0.512	0.375	0.250	0.258	0.216
Post-225 min (30 minutes post-MLD)								
Median	48.3	46.5	49.6	53.4	44.1	44.1	37.0	38.4
Interquartile range	44.0–50.8	44–53.9	48.4–54.6	48.9–56.2	44–46.2	42.2–48.6	36.3–39.8	36–40
Marginal mean (SE)	48.5 (1.5)	49.7 (1.5)	52.3 (1.5)	53.6 (1.2)	45.5 (0.9)	45.8 (0.9)	38.8 (0.7)	39.6 (0.8)
Mean % change from baseline	0.89	2.19	2.57	3.84	1.10	1.58	−1.29	−0.02
90% confidence interval	−1.45–3.23	0.07–4.30	0.67–4.47	2.63–5.05	−0.05–2.26	0.71–2.45	−3.04–0.46	−0.62–0.57
P value	0.531	0.090	0.026	0.001	0.116	0.003	0.224	0.950
Post-225 min (30 minutes post-MLD)								
Median	46.4	48.9	48.2	45.9	43.8	42.2	40.3	40.3
Interquartile range	43.8–48.8	44.7–50.4	43.9–51.5	43.9–48.9	41.2–44.1	40.4–45.2	39.4–40.4	37.9–41
Marginal mean (SE)	47.5 (1.5)	48.1 (1.6)	49.7 (1.3)	47.2 (1.3)	44.9 (1.1)	44.5 (1)	40.6 (0.9)	40.7 (0.9)
Mean % change from baseline	−0.08	0.62	−0.10	−2.59	0.51	0.25	0.47	1.02
90% confidence interval	−2.51–2.35	−1.64–2.89	−1.75–1.54	−4.06 to −1.12	−1.04–2.07	−1.78–2.27	−0.80–1.74	0.04–2.00
P value	0.957	0.651	0.917	0.004	0.589	0.843	0.545	0.089

MLD manual lymphatic drainage, *SE* standard error.
The final timepoint [post-225 min (30 minutes-post-MLD)] was assessed in the sitting position, while all prior timepoints were assessed in the head-down tilt position.

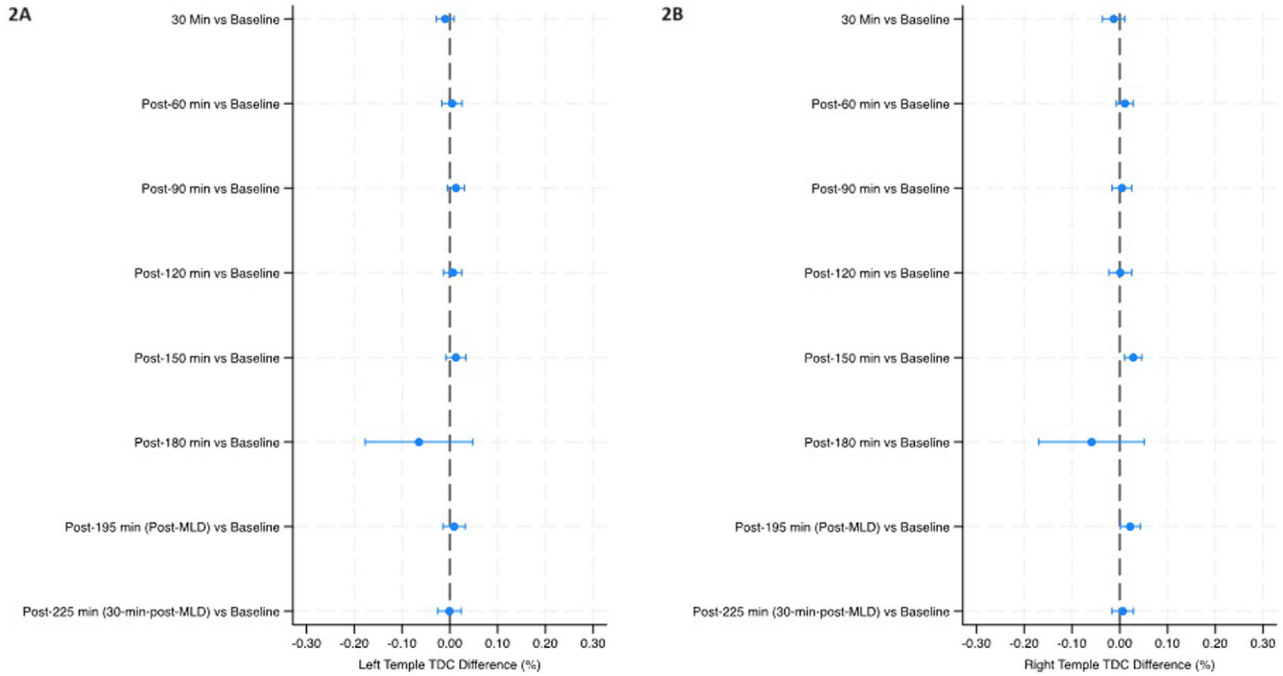

Fig. 2 | Tissue dielectric constant (TDC) measurements left and right temple. Mean percent change (90% Confidence Intervals) in tissue dielectric constant (TDC) from baseline over the course of the study in the left temple (2A) and right temple (2B). The final timepoint [post-225 min (30-min-post-MLD)] was assessed in the sitting position, while all prior timepoints were assessed in the head-down tilt position. Line indicates statistical difference, $p < 0.10$. MLD manual lymphatic drainage.

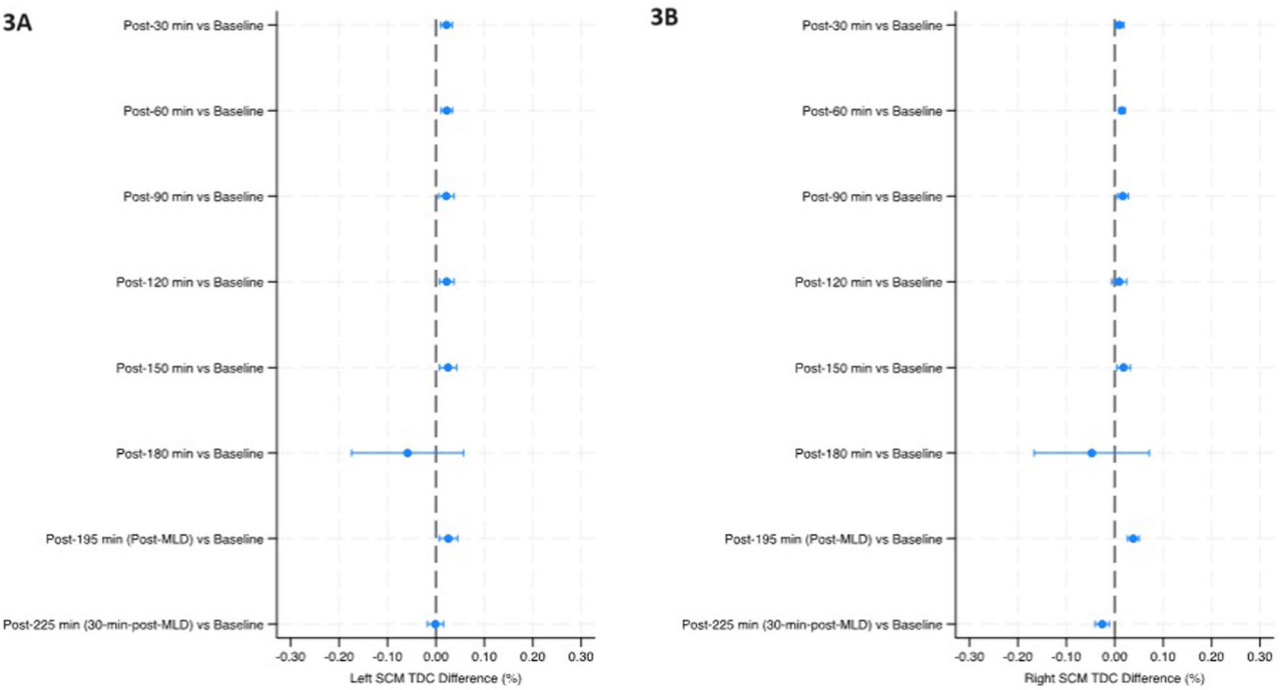

Fig. 3 | Tissue dielectric constant (TDC) measurements left and right sterno-cleidomastoid muscle. Mean percent change (90% Confidence Intervals) in tissue dielectric constant (TDC) from baseline over the course of the study in the left SCM (3A) and right SCM (3B). The final timepoint [post-225 min (30-min-post-MLD)] was assessed in the sitting position, while all prior timepoints were assessed in the head-down tilt position. Line indicates statistical difference, $p < 0.10$. MLD manual lymphatic drainage, SCM sternocleidomastoid.

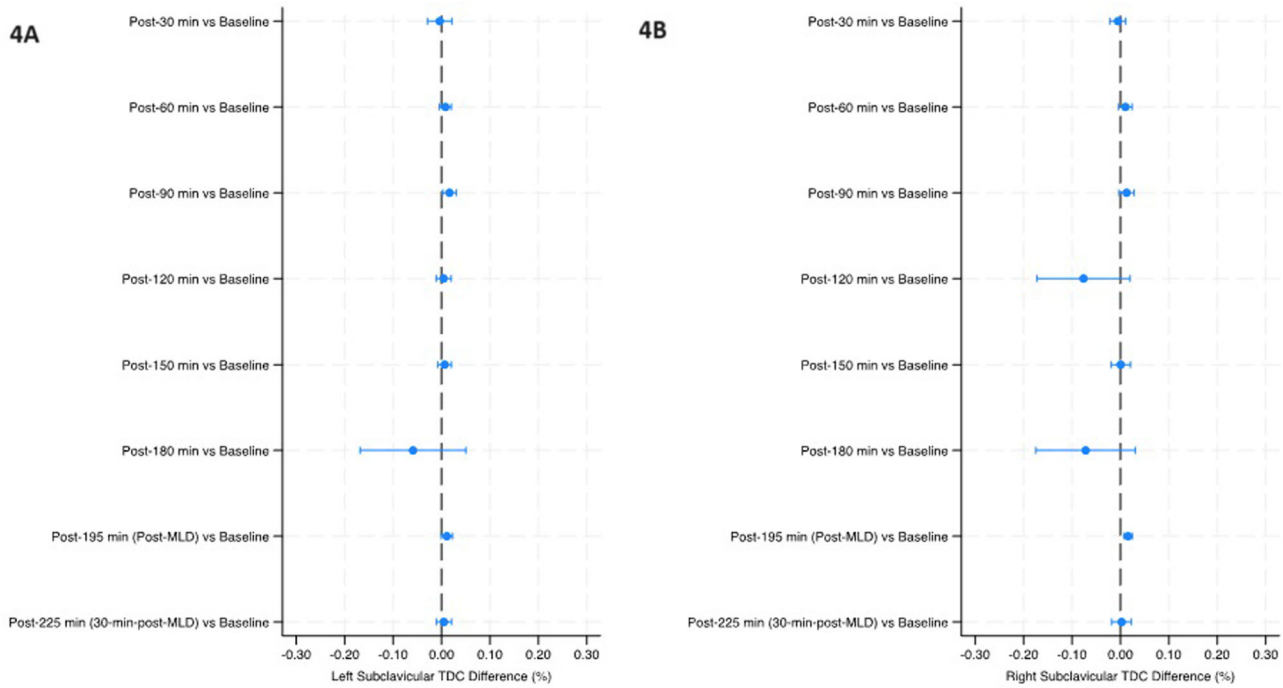

Fig. 4 | Tissue dielectric constant (TDC) measurements left and right subclavicular region. Mean percent change (90% Confidence Intervals) in tissue dielectric constant (TDC) from baseline over the course of the study in the left subclavicular region (4A) and right subclavicular region (4B). The final timepoint [post-225 min (30-min-post-MLD)] was assessed in the sitting position, while all prior timepoints were assessed in the head-down tilt position. Line indicates statistical difference, $p < 0.10$. MLD manual lymphatic drainage.

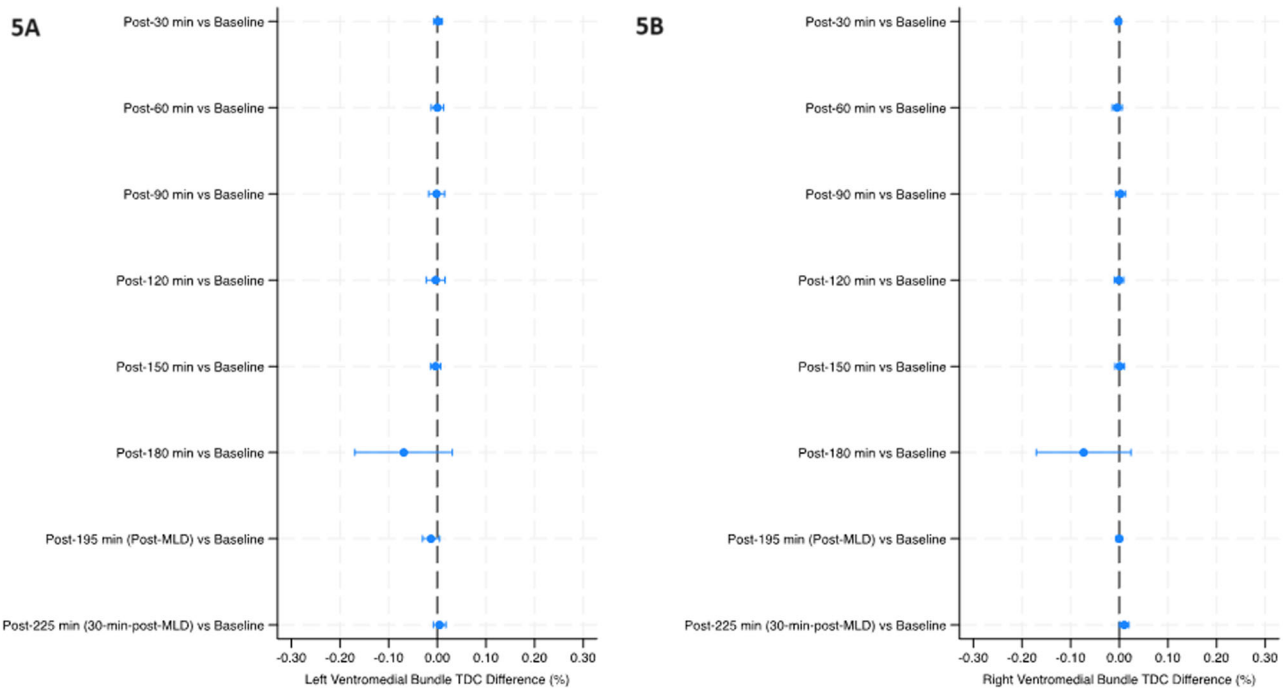

Fig. 5 | Tissue dielectric constant (TDC) measurements left and right ventromedial bundle region. Mean percent change (90% Confidence Intervals) in tissue dielectric constant (TDC) from baseline over the course of the study in the left ventromedial bundle region (5A) and right ventromedial bundle (5B). The final timepoint [post-225 min (30-min-post-MLD)] was assessed in the sitting position, while all prior timepoints were assessed in the head-down tilt position. Line indicates statistical difference, $p < 0.10$. MLD manual lymphatic drainage.

Table 3 | Summary of analysis of tissue oxygenation measurements (%) captured by near-infrared spectroscopy device at the knee, leg, and subclavian region

Timepoint	Medial knee		Proximal leg		Subclavian, frontal	
	Left, *n* = 13	Right, *n* = 13	Left, *n* = 13	Right, *n* = 13	Left, *n* = 13	Right, *n* = 13
Baseline						
Median, %	59	57	63	63	72	71
Interquartile range	56–64	56–62	60–67	59–66	68–76	69–73
Marginal mean (SE)	59.2 (1.8)	59.8 (1.8)	63 (1.1)	63.2 (1.4)	70.8 (2.1)	68.8 (2)
Post-30 min						
Median, %	55	55	60	57	68	67
Interquartile range	52–60	52–57	58–63	56–62	61–75	55–72
Marginal mean (SE), %	55.7 (1.5)	55.6 (1.9)	60.2 (2)	59.8 (2.2)	68.3 (2.7)	64.8 (2.7)
Mean % change from baseline	−3.49	−4.22	−2.79	−3.36	−2.55	−3.96
90% confidence interval	−5.33 to −1.65	−7.91 to −0.53	−5.75–0.16	−5.21 to −1.52	−4.48 to −0.62	−6.39 to −1.52
P value	0.002	0.060	0.120	0.003	0.030	0.008
Post-60 min						
Median, %	55	55	56	57	65	64
Interquartile range	49–58	52–57	55–63	52–63	58–74	57–69
Marginal mean (SE), %	55.4 (2.2)	55.7 (2)	58.2 (1.6)	57.4 (1.9)	65.9 (2.4)	63.1 (2.6)
Mean % change from baseline	−3.84	−4.12	−4.77	−5.71	−4.92	−5.63
90% confidence interval	−6.36 to −1.32	−7.15 to −1.09	−6.93 to −2.61	−8.88 to −2.53	−7.30 to −2.55	−8.34 to −2.91
P value	0.012	0.025	<0.001	0.003	0.001	0.001
Post-90 min						
Median, %	54	55	57	55	65	61
Interquartile range	49–58	51–58	55–58	54–59	59–70	53–70
Marginal mean (SE), %	54.6 (2)	54.2 (1.7)	57.2 (1.4)	55.9 (1.6)	64.9 (2.1)	62.1 (2.4)
Mean % change from baseline	−4.6	−5.59	−5.77	−7.22	−5.92	−6.65
90% confidence interval	−7.35 to −1.93	−8.08 to −2.61	−8.08 to −3.46	−9.04 to −5.41	−8.16 to −3.68	−9.10 to −4.19
P value	0.005	0.002	<0.001	<0.001	<0.001	<0.001
Post-120 min						
Median, %	54	56	60	57	68	64
Interquartile range	51–58	51–58	56–62	54–61	64–71	59–70
Marginal mean (SE), %	55.2 (1.9)	−4.60	58.8 (1.3)	58 (1.3)	67.0 (1.8)	63.7 (2)
Mean % change from baseline	−4.05	55.2 (1.5)	−4.12	−5.47	−3.83	−5.07
90% confidence interval	−7.28 to −0.83	−7.43 to −1.78	−6.52 to −1.71	−7.84 to −3.11	−6.02 to −1.63	−6.79 to −3.35
P value	0.039	0.007	0.005	<0.001	0.004	<0.001
Post-150 min						
Median, %	56	55	56	58	70	65
Interquartile range	50–63	50–59	54–60	54–61	64–73	60–71
Marginal mean (SE), %	55.6 (1.9)	54.4 (1.6)	57 (1.2)	58.1 (1.2)	67.5 (2.1)	64.4 (2.2)
Mean % change from baseline	−3.64	−5.42	−5.97	−5.02	−3.33	−4.40
90% confidence interval	−6.49 to −0.79	−8.69 to −2.16	−8.67 to −3.27	−7.51 to −2.54	−6.34 to −0.32	−5.90 to −2.90
P value	0.036	0.006	<0.001	0.001	0.069	<0.001
Post-180 min						
Median, %	55	53	57	55	63	61
Interquartile range	50–58	49–57	55–60	53–60	61–74	56–69
Marginal mean (SE), %	54.1 (1.9)	52.9 (1.6)	57 (1)	56.5 (1.4)	65.9 (2.2)	62.7 (2.1)
Mean % change from baseline	−5.14	−6.91	−5.98	−6.66	−4.89	−6.12
90% confidence interval	−7.62 to −2.66	−10.49 to −3.34	−8.53 to −3.44	−8.83 to −4.48	−7.99 to −1.78	−8.73 to −3.51
P value	0.001	0.002	<0.001	<0.001	0.010	<0.001
Post-195 min (post-MLD)						
Median, %	53	53	56	56	67	63
Interquartile range	50–57	50–56	53–60	51–61	63–72	61–69
Marginal mean (SE), %	52.5 (1.5)	52.3 (1.4)	56.2 (1.1)	56.1 (1.4)	66.4 (2.1)	63.3 (2.1)
Mean % change from baseline	−6.72	−7.5	−6.74	−7.09	−4.40	−5.44
90% confidence interval	−8.78 to −4.65	−10.12 to −4.89	−9.14 to −4.34	−9.40 to −4.77	−6.83 to −1.97	−8.06 to −2.81
P value	<0.001	0.001	<0.001	<0.001	0.003	0.001
Post-225 min (30 minutes post-MLD)						
Median, %	57	57	60	61	71	72
Interquartile range	55–61	54–60	57–63	59–65	68–74	67–73
Marginal mean (SE), %	56.3 (1.6)	57.2 (1.8)	60 (1.1)	61.7 (1.1)	71.7 (1.8)	69.8 (1.8)
Mean % change from baseline	−2.94	−2.67	−2.99	−1.45	0.85	0.98
90% confidence interval	−6.22–0.34	−5.67–0.33	−5.45 to −0.53	−3.73–0.84	−2.03 to −3.74	1.66 to −3.62
P value	0.141	0.143	0.046	0.298	0.626	0.543

MLD manual lymphatic drainage, *SE* standard error.
The final timepoint [post-225 min (30 minutes post-MLD)] was assessed in the sitting position, while all prior timepoints were assessed in the head-down tilt position.

Table 4 | Summary of analysis of tissue oxygenation measurements (%) captured by near-infrared spectroscopy device at the temporal region, venous angles, and forehead

Timepoint	Temporal lobe, frontal		Venous angle, frontal		Venous angle, lateral		Forehead
	Left, *n* = 12	Right, *n* = 12	Left, *n* = 13	Right, *n* = 12	Left, n = 12	Right, *n* = 13	*n* = 13
Baseline							
Median, %	75	74	72	69	77	74	77
Interquartile range	73–80	72–78	64–75	61–74	74–80	67–78	74–78
Marginal mean (SE)	76.7 (1.4)	74.5 (1.1)	70 (2.1)	67.1 (2.8)	75.8 (1.8)	72.9 (2.2)	75.1 (1.6)
Post-30 min							
Median, %	72	73	65	65	72	69	75
Interquartile range	71–77	69–76	61–70	62–68	63–76	63–75	69–76
Marginal mean (SE), %	73 (1.4)	72.7 (1.4)	65.1 (1.7)	63.6 (2.2)	70.9 (1.9)	69 (2.2)	73.1 (1.2)
Mean % change from baseline	−3.67	−1.78	−4.83	−3.46	−4.96	−3.90	−1.99
90% confidence interval	−6.04 to −1.29	−3.18 to	−7.18 to −2.47	−6.26 to −0.66	7.30 to −2.62	−5.61 to	−4.07–0.09
P value	0.011	−0.38 0.036	0.001	0.042	0.001	−2.19 <0.001	0.116
Post-60 min							
Median, %	72	71	65	61	70	69	72
Interquartile range	71–73	70–76	57–66	58–66	67–75	63–74	68–73
Marginal mean (SE), %	72 (0.9)	71.9 (1.2)	63.1 (2.1)	60.2 (2.2)	69.6 (1.7)	67.9 (2.3)	70.8 (1.1)
Mean % change from baseline	−4.67	−2.55	−6.86	−6.84	−6.20	−4.99	−4.34
90% confidence interval	−6.77 to −2.50	−4.48 to	−9.16 to −4.57	−9.99 to −3.68	−8.35 to −4.05	−7.39 to	−6.52 to −2.16
P value	<0.001	−0.62 0.030	<0.001	<0.001	<0.001	−2.58 0.001	0.001
Post-90 min							
Median, %	72	71	61	60	71	66	71
Interquartile range	70–74	69–72	57–70	57–70	64–75	61–72	67–73
Marginal mean (SE), %	71.3 (0.9)	71 (1.1)	63.2 (1.9)	61 (3)	69.9 (2.1)	67.3 (2.1)	69.9 (1.1)
Mean % change from baseline	−5.30	−3.48	−6.79	−6.04	−5.92	−5.58	−5.20
90% confidence interval	−7.61 to −3.00	−4.75 to	−8.79 to −4.79	−8.50 to −3.58	−8.57 to −3.28	−7.99 to	−7.32 to −3.07
P value	<0.001	−2.21 <0.001	<0.001	<0.001	<0.001	−3.17 <0.001	<0.001
Post-120 min							
Median, %	72	71	67	64	72	70	70
Interquartile range	70–73	68–72	63–71	60–68	71–76	65–74	66–73
Marginal mean (SE), %	71.6 (0.7)	70.7 (1)	66.2 (1.7)	62.8 (2.5)	71.9 (1.6)	67.9 (2.3)	69.9 (1.3)
Mean % change from baseline	−5.09	−3.84	−3.79	−4.31	−3.88	−4.98	−5.27
90% confidence interval	−7.30 to −2.89	−5.71 to	−5.93 to −1.66	−6.25 to −2.36	−6.18 to −1.57	−8.01 to	−7.93 to −2.62
P value	<0.001	−1.96 0.001	0.003	<0.001	0.006	−1.96 0.007	<0.001
Post-150 min							
Median, %	72	71	64	61	71	68	69
Interquartile range	70–74	68–72	59–70	57–71	67–74	64–73	66–72
Marginal mean (SE), %	71.4 (1.0)	70.2 (1.1)	64 (2.2)	61.1 (3.3)	70.2 (1.6)	69 (2)	69 (1.5)
Mean % change from baseline	−5.26	−4.27	−6.02	−6.01	−5.63	−3.81	−6.07
90% confidence interval	−6.86 to −3.67	−6.46 to	−8.96 to −3.07	−9.45 to −2.57	−8.19 to −3.07	−6.89 to	−8.72 to −3.43
P value	<0.001	−2.07 0.001	0.001	0.004	<0.001	−0.73 0.042	<0.001
Post-180 min							
Median, %	70	68	58	60	72	70	69
Interquartile range	66–72	66–74	55–74	55–74	69–76	65–74	65–73
Marginal mean (SE), %	69.1 (0.8)	69.2 (1.3)	62.3 (2.6)	58.4 (2.9)	71.3 (1.5)	68.9 (1.5)	68.7 (1.6)
Mean % change from baseline	−7.52	−5.29	−7.65	−8.63	−4.49	−3.97	−6.48
90% confidence interval	−9.94 to −5.10	−7.62 to −296	11.38 to −3.92	−11.78 to −5.47	−7.08 to −1.90	−7.30 to	−9.26 to −3.69
P value	<0.001	<0.001	0.001	<0.001	0.005	−0.63 0.051	<0.001
Post-195 min (post-MLD)							
Median, %	69	69	63	60	71	67	67
Interquartile range	68–70	67–72	54–65	57–66	66–72	62–71	65–72
Marginal mean (SE), %	69 (0.6)	68.7 (0.8)	60.5 (2.1)	58.8 (2.8)	68.5 (1.5)	66.5 (1.5)	67.4 (1.2)
Mean % change from baseline	−7.64	−5.78	−9.46	−8.28	−7.33	−6.32	−7.77
90% confidence interval	−10.08 to	−7.86 to	−12.04 to −6.68	−10.74 to −5.82	−9.90 to −4.77	−8.94 to	−10.46 to −5.08
P value	−5.20 <0.001	−3.70 <0.001	<0.001	<0.001	<0.001	−3.71 <0.001	<0.001
Post-225 min (30 minutes post-MLD)							
Median, %	69	69	71	69	66	69	66
Interquartile range	67–71	67–70	66–74	66–70	65–72	68–72	64–69
Marginal mean (SE), %	69.1 (0.8)	68.9 (0.9)	69.2 (1.6)	63.4 (1.7)	67.9 (1.4)	69 (1.1)	66.3 (1.1)
Mean % change from baseline	−7.53	−5.62	−0.84	−1.29	−7.90	−3.84	−8.680
90% confidence interval	−9.25 to −5.81	−7.25 to	−4.45–2.78	−2.34–4.91	−10.49 to	−6.92 to	−11.07 to −6.54
P value	<0.001	−4.00 <0.001	0.703	0.559	−5.32 <0.001	−0.76 0.040	<0.001

MLD manual lymphatic drainage, *SE* standard error.

The final timepoint [post-225 min (30 minutes post-MLD)] was assessed in the sitting position, while all prior timepoints were assessed in the head-down tilt position.

significantly decreased from baseline at each timepoint ($p < 0.001$), with the largest decrease observed following MLD therapy at 195-minutes [from 20.4 (0.8) to 16.4 (0.8), a 4.00% decrease, 90% CI: −5.33 to −2.67, $p < 0.001$]. Body temperature slightly decreased by ~0.1 °C from baseline at post-150 min thereafter ($p < 0.05$); however, the 90% CI nearly approached zero at each timepoint (Table 6).

Discussion

This is the first HDT spaceflight analog study, to our knowledge, in which dermal fluid shifts were evaluated using POC NIID, including NIRS, LWIT, and a lymphatic fluid scanner, with subsequent application of MLD techniques to stimulate dermal lymphatic function to mitigate cephalad fluid shifts.

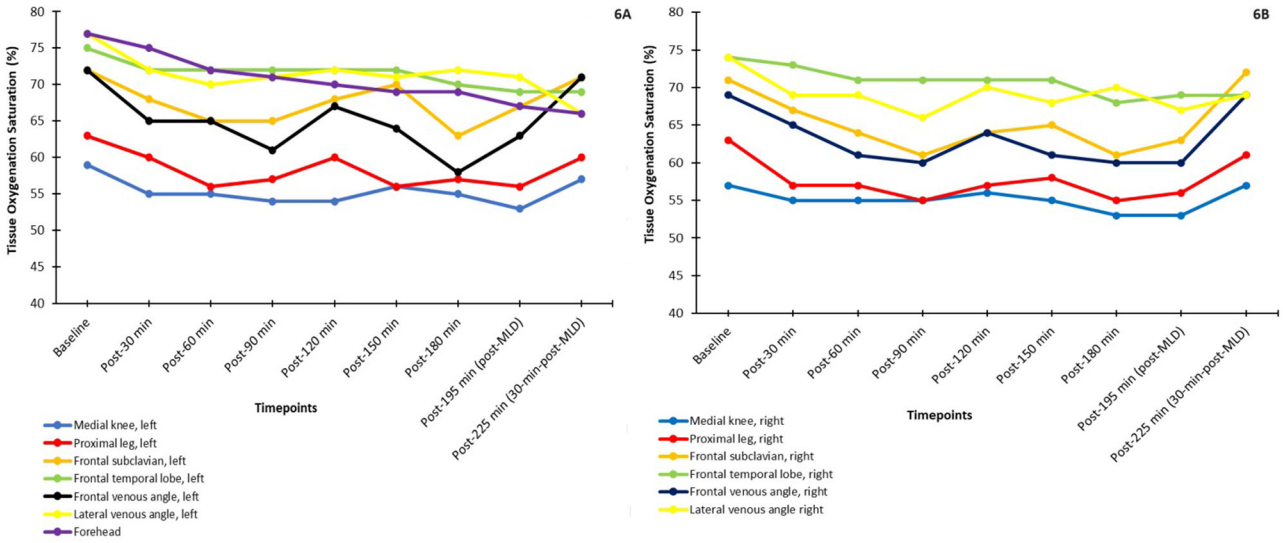

Fig. 6 | Median tissue oxygen saturation (%) levels, areas of interest, left and right side. Median tissue oxygen saturation levels (%) measured over the course of the study on the left side (6A) and right side (6B) of all areas of interest. Only the front (not the sides) of the forehead was measured, so it is included in **A** only. MLD manual lymphatic drainage.

In the HDT position, we would expect that fluid should shift away from the legs to the upper torso and head/neck[7]. In our small sample, the SCM muscle of the neck showed significant increases from baseline as soon as 30 minutes after assuming the HDT position, reflecting the initial cephalad fluid shift through post-150 min, while the legs were the most stable AOI until 180 minutes, when they saw a sudden (albeit anticipated) decrease (Table 2). The lymphangion contractility of the head and neck is simply less robust and primarily gravity dependent, while the legs have robust lymphangion contractility and respond well to subatmospheric pressure differences (i.e., the Guyton principle)[2]. After 180 minutes in the HDT position in our study, marginal means (but not necessarily medians) suddenly decreased at the neck, and this timepoint saw the largest percent change from baseline for all AOIs, albeit an insignificant change due to the sample size limitations (Table 2). Fifteen minutes of MLD appeared to reverse the change observed at 180 minutes, with values returning to or approaching baseline at post-195 min (Figs. 2–5). Because we analyzed fluid shifts through only 180 minutes in HDT prior to applying MLD, it is possible the timepoints analyzed were not as sensitive to imaging changes as anticipated, as the majority of fluid is redistributed after the first 6 hours (360 minutes) of microgravity[7]. In a previous study of 7 subjects, interstitial fluid pressures began to peak after 240 minutes in HDT the position[7]; we believe that the drastic change in variables analyzed after 180 minutes hours may be reflective of approaching peak fluid redistribution that becomes significant at 240 minutes.

Previous authors also have reported that just 30 minutes of bed rest resulted in 900 ml of fluid (likely venous blood) shifting away from the legs[38], and we saw a notable decrease in median (IQR) TDC levels in the right leg after only 30 minutes, from 38.5 (36.6–40.4) at baseline to 37.2 (37.00–40.2) at post-30 min (Table 2). However, the most important limitation of our TDC analysis was the very small sample size, which resulted in large SE values and overlapping 90% CIs that impacted statistical analysis. For example, this limitation rendered the noticeable drop in marginal mean TDC levels at post-180 min for all AOIs insignificant. On the other hand, the noticeable drop that only occurred in the right subclavicular site at post-120 min was also not significant and was likely an issue related to the sample size (Table 2, Fig. 4B).

We generally observed more noticeable changes in TDC in the right AOI compared to the left AOI. A change in fluid volume at AOI would alter the electrical resistance of that particular AOI segment, and so segmental leg resistance, or impedance, is observed to increase in the 6-degree HDT position[39]. Impedance could, therefore, serve as a proxy measure of fluid redistribution[39,40]. Fluid shifts on the left and right sides of the body are known to vary in the HDT position, with impedance greater on the right side, a trend that is more pronounced in the upper torso compared to the legs, but not always consistent[39,40]. Inconsistent torso findings may be a result of the motion-limitations of the HDT spaceflight analog, as spaceflight crew does not remain motionless in microgravity, and so it may not be appropriate to require subjects to refrain from movement in terrestrial models[39].

An increase in perfusion (Tables 3 and 4) and thermal energy (Table 5) at the neck was observed that appeared to resolve following MLD, while a decrease in perfusion and thermal energy was observed in the legs, with levels returning to baseline only when participants moved out of HDT to the sitting position. In the HDT position, we believe that fluid redistribution to the head/neck is driven by venous congestion, which would increase deoxygenated hemoglobin and decrease oxygenated hemoglobin, resulting in decreased tissue oxygenation (based on a ratio of the former to the latter) captured by NIRS. Significant changes in tissue oxygenation saturation levels have been reported as soon as 90–180 minutes after assuming HDT position[22,25,26]. In our study, tissue oxygenation levels showed fluctuation, but the largest (and most anticipated) decrease from baseline was observed at post-180 min, again likely reflecting the approach to the peak in alterations that would have been observed after 240 minutes[7]. MLD resulted in a noticeable increase in tissue oxygenation at most AOI, with values approaching baseline at post-195 min (Tables 3 and 4, Fig. 6), which would be expected, because venous congestion would have resolved immediately (whereas interstitial edema may still lag). In Fig. 6, with the exception of the right lateral venous angle, MLD appeared to be slightly more effective in resolving tissue oxygenation reductions on the right side of the body. This is likely because the right side is more easily congested (with its smaller lymphatic drainage basin compared to the left), as reflected in its lower tissue oxygenation levels in Tables 3 and 4.

The increased venous congestion in the head/neck region, would have increased thermal energy at these AOI, and so, the resulting temperature gradient would have been larger. With more venous congestion on the right side of the body, we would expect a shift in greater thermal energy on this side as well. Likewise the legs would have decreased thermal energy as a result of the cephalad shift. Figure 6 elegantly shows that right side of the head/neck had abnormally high (>+1 °C) temperature gradient

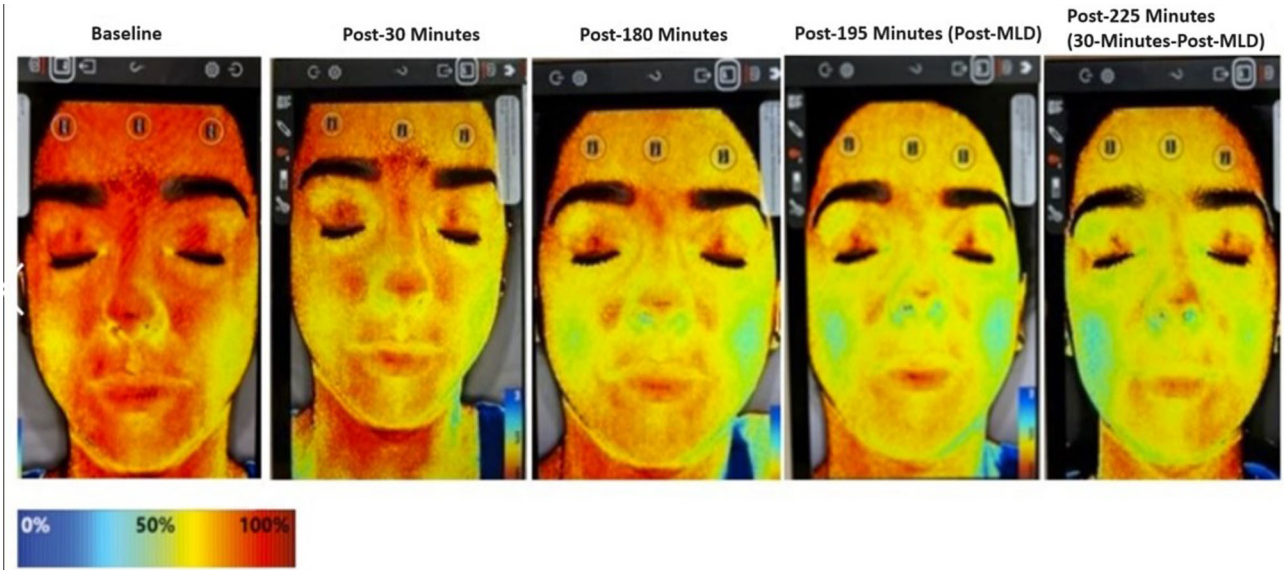

Fig. 7 | Near-infrared spectroscopy images of the head (face) and neck in a healthy, 28-year-old female subject. All assessments were taken while in head-down tilt (HDT) position, except for the post-225 min timepoint, when the subject was seated for 30 min. The color reference scale demonstrates the level of tissue oxygenation saturation on a percentage scale (oxygenation increases as levels approach red and decreases as levels approach blue). A visible reduction of tissue oxygenation levels proportional to the amount of time in spent in HDT position was observed. Interestingly, the tissue oxygenation visual levels of the neck appeared to increase over time while in the HDT position, but after manual lymphatic drainage (MLD) at both post-195 min in the HDT position and post-225 min in the sitting position, levels appeared to decrease in intensity.

Fig. 8 | Median tissue temperature gradient levels (°C) measured over the course of the study. MLD manual lymphatic drainage.

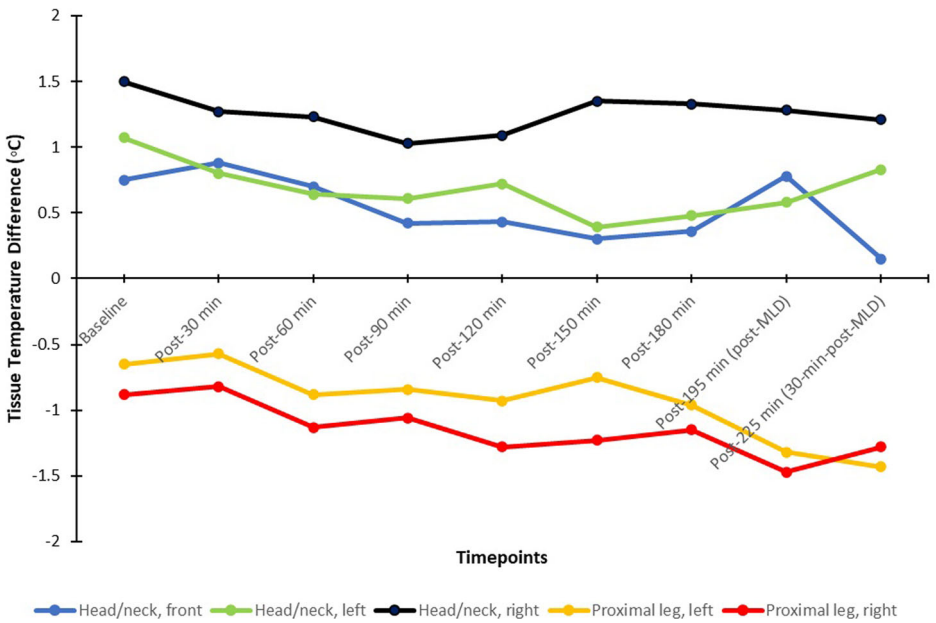

levels upon immediately assuming HDT position, while the right leg had abnormally lower temperature gradient levels (<−1 °C) after 1 hour in the HDT position. Anecdotally, increased heat signals on the right side of the neck compared to the left, though not quantifiable (Figs. 7 and 9) were visually noted with both thermography and NIRS, as ventromedial bundles did not increase in thermal patterns throughout the data collection, as expected, due to decreasing lower extremity venous pooling based on non-gravity-assisted positions. While our infrared images concentrated on gathering data from specific AOI, the visual color images of larger areas demonstrated thermal changes affected by position, time, and MLD techniques (Figs. 7 and 9). A 2023 report noted the right-side dominance of venous drainage in the head/neck region, and this may correlate with the nonvalidated visual findings noted in our study[41]. A further investigation could correlate our findings with venous duplex ultrasound to determine venous distention, which has been performed in both spaceflight analogs and true weightlessness[42].

With the exception of blood oxygenation, all other vitals changed over the course of the study (Table 6). Respiratory rate decreased, given that the participants were in a relaxing position. There was a decrease in body temperature due to the cooler room temperature set for subject's comfort. Blood pressure increased while heart rate decreased, due to the HDT positioning causing the cephalic fluid shift, which increases cardiac output, with an increased stroke volume leading to a slower (or unchanged) heart rate[6,7].

Table 5 | Summary of analysis of long-wave infrared thermography (LWIT) tissue temperature gradient data captured by LWIT and wound imaging device at different anatomic areas of interest (AOIs), based on an LWIT color thermal energy gradient scale from –7 °C to 7 °C for the AOI

Timepoint	Head/neck			Proximal leg	
	Front	Left	Right	Left	Right
Baseline					
Median	0.75	1.07	1.50	−0.65	−0.88
Interquartile range	0.02–1.15	0.77–1.22	1.37–1.73	−0.82 to −0.37	−1.20 to −0.63
Marginal mean (SE)	0.65 (0.17)	0.93 (0.12)	1.43 (0.12)	−0.56 (0.11)	−0.82 (0.13)
Post-30 min					
Median	0.88	0.80	1.27	−0.57	−0.82
Interquartile range	0.57–0.92	0.58–1.15	1.02–1.68	−0.90 to −0.20	−1.17 to −0.43
Marginal mean (SE)	0.79 (0.09)	0.88 (0.12)	1.25 (0.12)	−0.63 (0.16)	−0.81 (0.13)
Mean % change from baseline	0.14	−0.05	−0.18	−0.07	0.02
90% confidence interval	−0.11–0.39	−0.33 to −0.01	−0.35–0.24	−0.29–0.15	−0.19–0.23
P value	0.366	0.791	0.080	0.603	0.896
Post-60 min					
Median	0.70	0.64	1.23	−0.88	−1.13
Interquartile range	0.43–0.93	0.45–0.85	0.87–1.50	−0.93 to −0.22	−1.33 to −0.92
Marginal mean (SE)	0.65 (0.10)	0.65 (0.07)	1.14 (0.10)	−0.71 (0.12)	−1.09 (0.09)
Mean % change from baseline	0.00	−0.28	−0.29	−0.15	−0.27
90% confidence interval	−0.30–0.30	−0.46 to −0.09	−0.52 to −0.06	−0.38–0.08	−0.52 to −0.02
P value	0.995	0.016	0.037	0.298	0.081
Post-90 min					
Median	0.42	0.61	1.03	−0.84	−1.06
Interquartile range	0.20–0.70	0.05–0.72	0.82–1.46	−0.93 to −0.72	−1.30 to −0.83
Marginal mean (SE)	0.43 (0.12)	0.47 (0.14)	0.89 (0.24)	−0.75 (0.13)	−0.86 (0.20)
Mean % change from baseline	−0.23	−0.46	−0.54	−0.9	−0.04
90% confidence interval	−0.56–0.11	−0.79 to −0.13	−0.89 to −0.19	−0.52–0.15	−0.44–0.36
P value	0.267	0.023	0.011	0.364	0.874
Post-120 min					
Median	0.43	0.72	1.09	−0.93	−1.28
Interquartile range	0.22–0.58	0.27–0.93	0.68–1.47	−1.20 to −0.75	−1.68 to −1.03
Marginal mean (SE)	0.30 (0.13)	0.62 (0.11)	1.11 (0.15)	0.94 (0.10)	−1.33 (0.13)
Mean % change from baseline	−0.35	−0.31	−0.32	−0.38	−0.51
90% confidence interval	−0.68 to −0.02	−0.57 to −0.05	−0.52 to −0.12	−0.61 to −0.15	−0.79 to −0.23
P value	0.084	0.049	0.009	0.007	0.003
Post-150 min					
Median	0.30	0.39	1.35	−0.75	−1.23
Interquartile range	−0.02–0.57	0.07–0.65	1.07–1.60	−1.18 to −0.70	−1.53 to −0.90
Marginal mean (SE)	0.09 (0.19)	0.40 (0.11)	1.22 (0.13)	−0.89 (0.10)	−1.23 (0.13)
Mean % change from baseline	−0.56	−0.53	−0.21	−0.33	−0.41
90% confidence interval	−0.96 to −0.17	−0.82 to −0.25	−0.43–0.02	−0.57 to −0.08	−0.62 to −0.19
P value	0.018	0.002	0.131	0.027	0.002
Post-180 min					
Median	0.36	0.48	1.33	−0.96	−1.15
Interquartile range	0.00–0.68	0.08–0.80	0.95–1.75	−1.23 to −0.67	−1.43 to −1.02
Marginal mean (SE)	0.28 (0.16)	0.47 (0.12)	1.28 (0.15)	−1.01 (0.13)	1.23 (0.13)
Mean % change from baseline	−0.38	−0.46	−0.15	−0.45	−0.41
90% confidence interval	−0.70 to −0.05	−0.73 to −0.20	−0.39–0.08	−0.72 to −0.18	−0.74 to −0.08
P value	0.058	0.004	0.289	0.006	0.039
Post-195 min (Post-MLD)					
Median	0.78	0.58	1.28	−1.32	−1.47
Interquartile range	0.48–0.95	0.45–0.95	1.18–1.42	−1.43 to −0.87	−1.60 to −0.98
Marginal mean (SE)	0.63 (0.16)	0.68 (0.08)	1.35 (0.08)	−1.14 (0.12)	−1.39 (0.17)
Mean % change from baseline	−0.02	−0.25	−0.08	−0.58	−0.56
90% confidence interval	−0.30–0.26	−0.46 to −0.04	−0.31–0.14	−0.86 to −0.30	−0.86 to −0.27
P value	0.918	0.047	0.546	0.001	0.002
Post-225 min (30-minutes Post-MLD)					
Median	0.15	0.83	1.21	−1.43	−1.28
Interquartile range	−0.23–0.52	0.73–1.00	0.88–1.37	−1.69 to −1.02	−1.79 to −0.84
Marginal mean (SE)	0.19 (0.14)	0.84 (0.09)	1.21 (0.12)	−1.45 (0.15)	−1.30 (0.19)
Mean % change from baseline	−0.46	−0.09	−0.22	−0.89	−0.48
90% confidence interval	−0.79 to −0.14	−0.34–0.15	−0.44–0.01	−1.16 to −0.62	−0.83 to −0.12
P value	0.019	0.525	0.118	0.000	0.027

MLD manual lymphatic drainage, *SE* standard error.

The final timepoint [post-225 min (30-minutes-post-MLD)] was assessed in the sitting position, while all prior timepoints were assessed in the head-down tilt position. Scores are for all 15 participants.

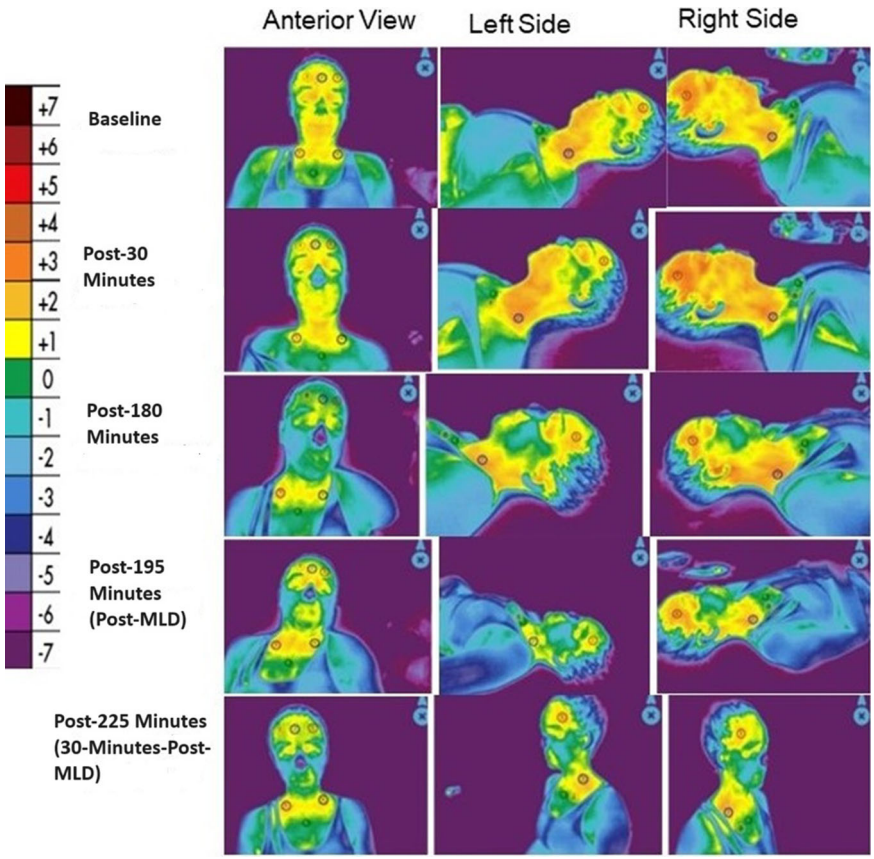

Fig. 9 | Long-wave infrared thermography (LWIT) images taken from an healthy, 28-year-old, female subject. All assessments were taken while in head-down tilt (HDT) position, except for the post-225 min timepoint, when the subject was seated for 30 min. The color reference scale measures thermal energy gradient in degrees Celsius, with increasing oxygenation approaching red and decreasing oxygenation; values >0 indicate hyperperfusion, while values <0 indicate hypoperfusion. In the above images, an initial increase in thermal energy emitted from the head and neck was greater on the right side, compared to the left, indicating increased perfusion or suspected venous engorgement over time in the HDT position. After manual lymphatic drainage (MLD) at post-195 min in the HDT position and post-225 min in the sitting position, there was a visual reduction of perfusion (or venous engorgement) in the head and neck towards normalcy.

This exploratory study was limited by its noncomparative, retrospective design, and we already discussed the major statistical limitations of our small sample size. This sample size was a reflection of the challenge of volunteer participation, as maintaining a strict HDT position over time may be uncomfortable, induce headaches, and severely limit mobility. Generalizing the findings of our volunteers to highly trained astronauts may also be a limitation, but we controlled for possibilities of medical history that could impact the study variables by only including a young and (self-reported) healthy population. However, activities, such as exercise, which can activate lymphatic function that may then persist for 60–240 minutes, were not restricted. Entering a cool building from a warm, humid external environment (the study was performed in Ft. Lauderdale, Florida) may have also potentially impacted imaging results, but subjects sat for 15 minutes upon arrival to the study site to acclimate to the ambient temperature prior to positioning and imaging. There is a small possibility that having a predominantly female population (11/15 subjects) may have introduced some bias to our results, as females have less total body water (the weighted mean tissue water content) than men (50% vs 60%)[43], and they have reduced blood oxygenation, muscle mass, oxidative potential, and capillary density compared to males[44].

Our NIID protocol was limited by not performing a controlled baseline assessment in the sitting position prior to assuming HDT. However, our baseline assessment was taken immediately (1 minute) after assuming HDT and provided an appropriate measurement to demonstrate fluid redistribution over time.

We also did not perform NIID during MLD, and we do not know what the repeated or long-term effects of MLD may have in simulated microgravity. Near-infrared fluorescence lymphatic imaging (NIRFLI) could have important correlative benefit for determining dermal lymphatic function. NIRFLI collects NIR fluorescent signals emanating from the lymphatics following the off-label administration of indocyanine green (ICG) and can be administered with concurrent MLD to assess changes in fluid flow[45]. NIRFLI was used in an HDT model to evaluate the effect of gravity on deep cervical lymphatic flow via palatine tonsil injection of ICG[46]. While subjects were in the HDT position, NIRFLI demonstrated that lymphatic drainage shared pathways with cerebral spinal fluid outflow that are dependent upon gravity and are impaired when subjected to short-term HDT. Of significance, NIRFLI determined lymphatic contractile rates following intradermal ICG injections of the lower extremities increased under the influence of gravity, regardless of force direction (sitting down or HDT). The implications of these outcomes provided evidence for the role of a lymphatic contribution in SANS[46].

Our LWIT and NIRS analyses were limited by the absence of advanced medical imaging software that more comprehensively quantifies and validates changes of the pixel data points generated by each image[47] (Figs. 9 and 8). Trained and experienced imagers visually analyzed these images in the current study, but this software will be needed for future study for definitive validation and image comparisons that are not purely subjective. Additionally, the data points or AOIs for the NIRS and LWIT devices were hand-selected for analysis, which may have led to subtle variation in area of interest or inter-rater error.

Importantly, despite the study limitations, this exploratory study demonstrated the feasibility of NIID for the immediate and continuous monitoring of fluid shifts experienced in weightlessness and that MLD appeared to reverse trends in fluid redistribution that were more prominently observed after 180 minutes in the HDT spaceflight analog. A follow-up comparative study of a larger sample size with a 6-hour (360-minute) time horizon is warranted to confirm our preliminary findings.

This proof-of-concept study piloted the use of innovative NIID to assess fluid redistribution at point of care during a validated spaceflight analog and supported the potential use of MLD to mitigate fluid shifts. A lymphatic fluid scanner, NIRS, and LWIT documented fluid redistribution with altered perfusion and thermal energy in the head/neck, upper torso, and legs in simulated microgravity; changes were particularly noticeable

Table 6 | Summary of available vitals data and analysis (n = 15)

Timepoint	Heart rate	Systolic blood pressure	Diastolic blood pressure	Respiratory rate	Body temperature, °C	Blood oxygen levels, %[a]
Baseline						
Median (IQR)	71.0 (64.0–77.0)	119.0 (113.0–124.0)	71.0 (69.0–77.0)	20.0 (18.0–22.0)	36.7 (36.6–36.8)	98.0 (96.0–99.0)
Marginal mean (SE)	70.5 (2–5)	118.8 (2.3)	71.9 (1.4)	20.4 (0.8)	36.7 (0)	97.4 (0.5)
Post-30 min						
Median (IQR)	66.0 (60.0–73.0)	117.0 (111.0–123.0)	75.0 (71.0–78.0)	18.0 (16.0–20.0)	36.7 (36.7–36.8)	98.0 (96.0–99.0)
Marginal mean (SE)	66.1 (2.5)	117.8 (2.3)	74.5 (1.4)	17.7 (0.8)	36.7 (0)	97.4 (0.6)
Mean % change from baseline	−4.47	−1.00	2.60	−2.66	0.05	0.000
90% confidence interval	−7.55 to –1.38	−5.24–3.24	−0.53–5.73	−3.99 to −1.34	−0.02–0.11	−0.009–0.010
P value	0.017	0.698	0.172	0.001	0.218	0.981
Post-60 min						
Median (IQR)	65.0 (59.0–71.0)	116.0 (111.0–118.0)	75.0 (71.0–77.0)	16.0 (14.0–20.0)	36.7 (36.6–36.8)	98.0 (98.0–99.0)
Marginal mean (SE)	65.4 (2.5)	116.4 (2.3)	75.1 (1.4)	16.5 (0.8)	36.7 (0)	97.7 (0.5)
Mean % change from baseline	−5.13	−2.40	3.13	−3.86	−0.01	0.003
90% confidence interval	−8.22 to −2.05	−6.64–1.84	0.00–6.27	−5.19 to −2.54	−0.07–0.06	−0.005–0.011
P value	0.006	0.352	0.100	<0.001	0.850	0.519
Post-90 min						
Median (IQR)	63.0 (58.0–67.0)	121.0 (119.0–126.0)	78.0 (71.0–80.0)	16.0 (14.0–18.0)	36.6 (36.6–36.9)	99.0 (97.0–99.0)
Marginal mean (SE)	63.7 (2.5)	122.7 (2.3)	75.5 (1.4)	15.9 (0.8)	36.7 (0)	97.4 (0.6)
Mean % change from baseline	−6.87	3.87	3.60	−4.53	0.02	0.000
90% confidence interval	−9.95 to −3.78	−0.37–8.10	0.47–6.73	−5.86 to −3.21	−0.05–0.08	−0.006–0.006
P value	<0.001	0.133	0.059	<0.001	0.636	0.943
Post-120 min						
Median (IQR)	63.0 (57.0–74.0)	118.0 (111.0–128.0)	76.0 (73.0–83.0)	16.0 (14.0–18.0)	36.6 (36.6–36.7)	98.0 (97.0–99.0)
Marginal mean (SE)	64.4 (2.5)	121.7 (2.3)	78.3 (1.4)	16.7 (0.8)	36.6 (0)	97.4 (0.6)
Mean % change from baseline	−6.13	2.93	6.33	−3.73	−0.07	0.000
90% confidence interval	−9.22 to −3.05	−1.30–7.17	3.20–9.47	−5.06 to −2.41	−0.14 to −0.01	−0.009–0.010
P value	0.001	0.255	0.001	<0.001	0.058	0.955
Post-150 min						
Median (IQR)	63.0 (56.0–75.0)	121.0 (114.0–127.0)	79.0 (75.0–81.0)	16.0 (14.0–16.0)	36.6 (36.5–36.7)	99.0 (98.0–99.0)
Marginal mean (SE)	63.6 (2.5)	120.0 (2.3)	78.1 (1.4)	15.6 (0.8)	36.5 (0)	98 (0.4)
Mean % change from baseline	−6.93	1.20	6.13	−4.80	−0.13	0.006
90% confidence interval	−10.02 to −3.85	−3.04–5.44	3.00–9.27	−6.13 to −3.47	−0.19 to −0.07	−0.002–0.013
P value	<0.001	0.641	0.001	<0.001	0.001	0.224
Post-180 min						
Median (IQR)	58.5 (54.0–71.0)	122.0 (115.0–122.0)	76.0 (73.0–80.0)	16.0 (14.0–18.0)	36.6 (36.6–36.6)	99.0 (98.0–99.0)
Marginal mean (SE)	62.6 (2.5)	122.4 (2.3)	76 (1.4)	15.8 (0.8)	36.6 (0)	98.2 (0.4)
Mean % change from baseline	−7.90	3.62	4.08	−4.56	−0.12	0.008
90% confidence interval	−11.04 to −4.75	−0.70–7.94	0.89–7.27	−5.91 to −3.21	−0.18 to −0.05	−0.001–0.017
P value	<0.001	0.168	0.036	<0.001	0.003	0.122
Post-195 min (Post-MLD)						
Median (IQR)	67.0 (60.0–77.0)	119.0 (116.0–127.0)	82.0 (77.0–87.0)	16.0 (16.0–18.0)	36.6 (36.5–36.6)	99.0 (98.0–99.0)
Marginal mean (SE)	66.7 (2.5)	121.8 (2.3)	81.4 (1.4)	16.4 (0.8)	36.6 (0)	98 (0.4)
Mean % change from baseline	−3.80	3.00	9.47	−4.00	−0.11	0.006
90% confidence interval	−6.88 to −0.72	−1.24–7.24	6.33–12.60	−5.33 to −2.67	−0.18 to −0.05	−0.001–0.012
P value	0.043	0.244	<0.001	<0.001	0.003	0.178
Post-225 min (30 minutes–Post-MLD)						
Median (IQR)	60.0 (56.0–75.0)	123.0 (119.0–132.0)	80.0 (76.0–85.0)	16.0 (14.0–18.0)	36.6 (36.5–36.7)	99.0 (98.0–99.0)
Marginal mean (SE)	66.7 (2.5)	125.4 (2.3)	80.3 (1.4)	15.3 (0.8)	36.6 (0)	98.2 (0.3)
Mean % change from baseline	−7.20	6.60	8.33	−5.07	−10.	0.01
90% confidence interval	−10.26 to −4.14	2.52–10.68	5.21–11.45	−6.41 to −3.72	−0.16 to −0.03	−0.00–0.02
P value	0.000	0.008	0.000	0.000	0.010	0.111

IQR interquartile range, *MLD* manual lymphatic drainage, *SE* standard error.

[a]Measured using pulse oximeter.

The final timepoint [post-225 min (30-minutes post-MLD)] was assessed in the sitting position, while all prior timepoints were assessed in the head-down tilt position.

Table 7 | Protocol used for noninvasive imaging devices

Anatomic site no.	Near-infrared spectroscopy anatomic sites	Long-wave infrared and wound imaging anatomic sites	Lymphatic fluid scanner anatomic sites
1	Forehead: front of face (forehead to chin), reference tip of nose	Front of head/neck: front of face, xiphoid to head, central point sternum	Left temple
2	Left side of frontal subclavian region: anterior neck to sternal notch, head slightly extended, reference at sternal notch	Left side of head/neck, mid-deltoid to top of head, central point sternum	Right temple
3	Right side of frontal subclavian region: anterior neck to sternal notch, head slightly extended, reference at sternal notch	Right side of head/neck, mid-deltoid to top of head, central point sternum	Left mid-SCM
4	Left side of frontal venous angle	Left leg: proximal thigh to mid-lower legs, central point left anterior lateral proximal thigh	Right mid-SCM
5	Right side of frontal venous angle	Right leg: proximal thigh to mid-lower legs, central point right anterior lateral proximal thigh	Left subclavicular
6	Left, lateral side of venous angle: side of head/neck with 45 degrees neck/rotation/extension, reference at venous angle	N/A	Right subclavicular
7	Right, lateral side of venous angle: side of head/neck with 45 degrees neck/rotation/ extension, reference at venous angle	N/A	Left ventromedial bundle
8	Proximal leg: left ventromedial bundle, reference medial knee	N/A	Right ventromedial bundle
9	Proximal leg: right ventromedial bundle, reference medial knee	N/A	N/A

N/A not applicable, *SCM* sternocleidomastoid muscle.

after 180 minutes in the HDT position. In many affected areas, MLD appeared to have reversed trends, allowing for levels to return to or approach baseline after only 15 minutes of therapy. A larger, controlled study that uses NIID to analyze fluid shifts, perfusion changes, and temperature differentiation at up to 6 hours (360 minutes) during which MLD would be administered would be ideal to confirm our preliminary findings. MLD may prove to be an effective countermeasure used preflight, during flight, and postflight to manage and/or restore fluid shifts experienced during weightlessness.

Ultimately, NIID assessment could help establish baseline measurements to compare similar measurements in true weightlessness. Ideally, NIID will help guide or establish countermeasures specifically to address fluid shifts preflight, during early and late spaceflight, and postflight conditions, with the potential to have significant "spinoff" applications for fluid shift recognition in wound care and lymphedema clinics to improve outcomes through recognition and improved treatment protocols. NIID could also assist in personalized precision application of countermeasures, as it is increasingly understood that lymphatic function is likely to be variable from individual to individual[48]. The imaging modalities are light weight/low mass units that can swiftly acquire repeatable imaging shortly after entering weightlessness and over the crucial 2–7 days the crew members acclimate to the fluid redistribution; they allow for ground-based, remote assessment; and they do not require dye injections, radiation exposure, or significant training. The images could also be remotely assessed by ground-based experts for interpretation, as authors have done with ultrasound images[42]. In this time-limited HDT analog study, NIID demonstrated to have high potential for continuous monitoring for terrestrial models and in true weightlessness and supported the potential countermeasure use of MLD to mitigate fluid shifts. Further investigation is warranted to confirm these findings in a larger, controlled population.

Methods

Study design

In 2022, our university physical therapy department experimented with the novel use of NIID in the HDT position on healthy students with no known lymphatic dysfunction to analyze lymphatic flow, perfusion, and tissue temperature gradient in a validated spaceflight analog. To participate, students could not be on blood pressure or vasodilation medications, and they could not use any form of nicotine. After 180 minutes of being in the HDT position, some of these students also underwent 15 minutes of MLD while still in the HDT position. We performed a retrospective chart review of those students who underwent MLD while in the HDT position. There were 30 students who underwent NIID imaging in the HDT position from 6 April 2022, through August 15, 2022, 15 of whom (50%) also had MLD in the HDT position. All 15 students were included in this retrospective analysis.

The primary endpoints included: fluid shifts measured by a lymphatic fluid scanner and defined as percent change in TDC from baseline; perfusion changes, as defined by percent change in tissue oxygenation from baseline captured by NIRS; and percent change in tissue temperature gradient from baseline captured by LWIT; with all endpoints measured in 30-minute intervals from baseline through 225 minutes (with subjects in the HDT position from baseline to 195 minutes, undergoing MLD from 181 to 195 minutes, and in the sitting position from 196 to 225 minutes). Additional endpoints analyzed were changes in vitals, including heart rate, systolic blood pressure, diastolic blood pressure, blood oxygenation (measured by pulse oximeter), respiration rate, and body temperature.

Inclusion and ethics statement

This research project included local researchers throughout the entire study process, was locally relevant, and was performed in collaboration with local partners. Prior research on this topic, both locally and regionally, was taken into account in the literature review performed for the study rationale and interpretation of analysis. All roles and responsibilities were agreed amongst collaborators prior to study initiation, and the capacity-building of students as coinvestigators and coauthors was involved. This project would not have been severely restricted or prohibited in the study setting. The research did not result in stigmatization, incrimination, discrimination, or personal, safety, or security risk to subjects. Health risk to subjects was minimal and included nasal congestion and headache as a consequence of fluids becoming congested in the head during the 3-hour HDT position prior to MLD. Vitals were monitored during this time and investigators asked subjects how they were feeling and what they were experiencing to minimize discomfort. This study adhered to the Declaration of Helsinki and all relevant ethical regulations. The Nova Southeastern University IRB approved the study protocol (No. 2022-124), which was registered on clinicaltrials.gov (NCT06405282). Subjects provided their written informed consent to participate in this study. They also provided their written informed consent for publication, including the publication of their identifiable images.

There was no calculation for the sample size for this exploratory, pilot retrospective analysis. The sample size was determined from chart review and based on the number of subjects who underwent MLD therapy while in the HDT position.

Table 8 | Manual lymphatic drainage (MLD) protocol administered to the head, neck, and thorax for 15 minutes, while in the head-down tilt position

Type of MLD treatment	Anatomic region	Description	No. of times performed[a]
Central decongestion and priming of the system	Venous angle	• Stimulated supraclavicular nodes/venous angle by hooking fingers bilaterally over clavicle using fingertips/pads	10
	Neck	• Stimulated neck by bilaterally stretching forward and distal toward venous angle	10
	Abdominal		
	Umbilicus/ abdominal area	• Performed thoracic duct/diaphragmatic breathing by teaching subject how to belly breathe and resist diaphragmatic breathing	5
	Cisterna chyli	• Deep abdominal technique over superior to umbilicus/below xiphoid; coordinated with diaphragmatic breathing, resisted a little more with each exhalation (if the aortic pulse was felt, held at that level for remaining cycles)	5
	Iliac nodes and lumbar trunks	• Found iliac crest, moved medially to soft area, and provided wave-like motion toward umbilicus, right and left side	5
	Axillary nodes	• Stimulated the axillary nodes ○ Right and left cephalic vasorum	10 5
Short neck treatment	Neck/shoulder	• Effleurage starting at the sternal notch following the clavicle to acromion process performed on both sides	3
		• Modified stationary circles in the supraclavicular fossa, stimulating the venous angle	5
		• Stationary circles on the lateral cervical triangle bilaterally	5
		• Stationary circles over the shoulder collectors on two locations on each side of the neck ○ First position closer to the neck, moving fluid away from neck toward axillary nodes ○ Second position distal over the acromion processes, deviating towards axillary nodes	5 5
		• Stationary circles pre- and retroauricular lymph nodes bilaterally	5
		• Reworked bilateral lateral cervical triangle bilaterally	5
		• Stationary circles submandibular area	5
		• Reworked bilateral lateral cervical triangle bilaterally	5
		• Stationary circles over axillary lymph nodes, each side ○ Right and left cephalic vaso vasorum	5 5
		• Reworked bilateral shoulder collectors in 2 locations (2D)	5
Facial MLD	Face	• Effleurage in 3 pathways ○ Lips to mandible ○ Nose to mandible ○ Forehead to in front of ear	5 5 5
		• Stationary circles on submandibular lymph nodes, both sides	5
		• Stationary circles on the lateral cervical triangle on both sides	5
		• Alternating stationary circles on face with fingertips over the edge of the mandible on each side of subject's mouth, hands parallel to sagittal watershed	5
		• Alternating stationary circles on face with hands moving slightly distal (away from neck) with fingertips pointing to edge of lips	5
		• Stationary circles on submandibular lymph nodes,	5
		• Stationary circles over the lateral cervical triangle on both sides	5
		• Alternating stationary circles on the bridge of the nose	5
		• Alternating stationary circles over cheeks	5
		• Alternating stationary circles with fingers pointing to edge of lips	5
		• Alternating stationary circles with fingertips over the edge of mandible	5
		• Stationary circles over the submandibular lymph nodes	5
		• Stationary circles on the lateral cervical triangle on both sides	5
		• Alternating stationary circles over upper and lower eyelids (if subject was not wearing contacts, otherwise needed to treat upper, then lower eyelids)	5
		• Alternating stationary circles to eyebrows medial to lateral	5
		• Forehead alternating stationary circles from midforehead to ears	5
		• Crown alternating stationary circles to ears	5
		• Stimulated pre- and retroauricular lymph nodes bilaterally	5
		• Stationary circles over the lateral cervical triangle on each side	5
		• Final effleurage on both sides of face	5
Venous angle	Venous angle	• Stimulated the nodes and connections between internal jugular and subclavian veins by gentle pumping technique behind the clavicles	10

[a]If both sides indicated in description, then the number of times refers to the number of times performed on each side.

MLD techniques are listed in chronological order of treatment administration.

Procedures

There were three different imaging devices that were donated in kind for use in this study and returned to manufacturers upon completion. A lymphatic fluid scanner (LymphScanner, Delfin Technologies, Miami, FL, USA) captured moisture readings and tissue edema by measuring TDC values at eight distinct AOI (including six of the head/neck region and two of the legs, as summarized in Table 7).

A NIRS device (SnapShotNIR, Kent Imaging, Calgary, Canada) captured perfusion changes by measuring tissue oxygenation, specifically a ratio of oxygenated and deoxygenated hemoglobin. The images were taken at 9 distinct anatomic locations summarized in chronological order in Table 7 (7 images of the head/neck region and 2 of the legs). Each image generated by NIRS has a reference color scale, representing tissue oxygenation saturation levels in percentages. A decrease in perfusion is noted as the value moves towards 0.

A long-wave infrared and wound imaging device (WoundVision Scout, WoundVision, Indianapolis, IN) captured 5 thermal images also at 5 distinct anatomic sites (three of the head/neck region and two of the legs) measuring physiological temperature differentiation (Table 7). LWIT measures the levels of thermal energy emitted from the human body because of physiological responses, which are translated to temperature gradients. Each thermal image has a reference long-wave LWIT color thermal energy gradient scale from −7 °C to 7 °C for the AOI. Normal thermal differentiation compared to surrounding tissue is in the range of −1 °C to +1 °C[49]. A reading >0 °C is considered hyperperfused or warmer, while <0 °C is considered hypoperfused or cooler.

Prior to NIID imaging, subjects arrived at a predesignated room for assessment and data collection. Subjects acclimated to the room and ambient temperature by sitting quietly for 15 minutes before assuming the HDT position. Vitals were taken and monitored at baseline and every 30 minutes through the end of each imaging session. Participants disrobed down to their shorts (women also wore sports bras) and positioned themselves in HDT using an inversion table (Fitspine XC5 Inversion Table, Bonney Lake, WA, USA). The table was first locked into place to allow them to position themselves correctly, and their ankles were secured prior to being placed in a 6-degree HDT position, as indicated by the table and confirmed using a smartphone inclinometer app (Inclinometer and Bubble Level, EzeShare File Transfer).

Four trained imagers participated in this study and followed the imaging protocol summarized in Table 7. One of the 4 imagers took baseline assessments using the NIID 1 minute after assuming the HDT position. Reassessments were performed every 30 minutes thereafter through 180 minutes. Each image acquisition was performed in 15 to 30 seconds. After 180 minutes in the HDT position, subjects remained in position while receiving 15 minutes of MLD to the head, neck, and upper torso. Table 8 describes the established MLD protocol, which involved central decongestion and priming of the system (stimulation of terminus and nodes), short neck treatment, facial MLD, and therapy applied to the venous angle. Immediately post-MLD (195 minutes after baseline assessment), reassessment with the devices occurred. Subjects then were placed in a sitting position to simulate their return to normal gravity from spaceflight analog positioning, allowing permissive gravity-assisted drainage of the head, neck, and upper torso. A follow-up reassessment was taken with the devices 30 minutes after MLD (225 minutes after baseline assessment) to assess potential changes and resolution of any symptoms experienced in any of the positions.

Data collection and analysis

All data, including patient characteristics, were transcribed to an Excel spreadsheet. Exploratory analysis comprised descriptive statistics to summarize baseline characteristics in the study cohort. Descriptive statistics were reported as frequencies with percentages for categorical variables and medians with IQRs for continuous variables. Beta regression was used to analyze marginal means with robust-clustered SEs to examine within-group change in TDC and tissue oxygenation saturation by timepoint. The beta distribution is a continuous probability distribution that uses the interval [0,1], making it a suitable distribution for the random behavior of percentages. A mixed, random-effect model was used to examine within-group change in vital statistics and LWIT at AOI. As 5 LWIT measurements were taken per position (front, left side, and right side of head/neck and left and right legs), the mean was compared between the 5 measurements. In all models, the fixed effects were timepoint ["Baseline", "Post-30 min", "Post-60 min", "Post-90 min", "Post-120 min", "Post-150 min", "Post-180 min", "Post-195 min (Post-MLD)", "Post-225 min (30-minutes-post-MLD)"]. All analyses used robust-clustered SEs to account for the violation of observation independence and homoscedasticity. Bounded data, such as percentages, often give rise to uncorrectable skewness and heteroscedasticity, and we needed to account for the correlated nature of the repeated measures. We used Dunnett's test to compare change against the baseline timepoint. Outcomes are reported as means with 90% CIs. Hypothesis testing was all two-sided, where significance was found at $p < 0.10$ to balance Type 1 and Type 2 error rates for our given sample size. Following the work of Maier and Lakens[50], increasing the Type 1 error rate from 0.05 to 0.10 reduced the Type 2 error rate from 0.20 to 0.12 and the combined error rate from 0.12 to 0.10. All statistical analyses were completed using available packages in R version 4.0.3 or higher (R Foundation, Vienna, Austria) and STATA 18.1 (College Station, TX, USA).

Data availability

The datasets used and/or analyzed during the study are available from the corresponding author on reasonable request.

Received: 3 September 2023; Accepted: 19 September 2024;
Published online: 03 October 2024

References

1. Ong, J., Lee, A. G. & Moss, H. E. Head-down tilt bed rest studies as a terrestrial analog for spaceflight associated neuro-ocular syndrome. *Front. Neurol.* **12**, 648958 (2021).
2. Guyton, A. C., Granger, H. J. & Taylor, A. E. Interstitial fluid. *Physiol. Rev.* **51**, 527–563 (1971).
3. Gashev, A., Delp, M. & Zawieja, D. Inhibition of active lymph pump by simulated microgravity in rats. *Am. J. Physiol. Heart Circ. Physiol.* **290**, H2295–H2308 (2006).
4. Stepanek, J., Blue, R. S. & Scott, P. Space medicine in the era of civilian spaceflight. *N. Eng. J. Med.* **380**, 1053–1060 (2019).
5. Thirsk, R. B. Health care for deep space explorers. *Ann. Icrp.* **49**, 182–184 (2020).
6. Jagtap, S. et al. Response of cardiac pulse parameters in humans at various inclinations via 360° rotating platform for simulated microgravity perspective. *NPJ Microgravity* **9**, 54 (2023).
7. Parazynski, S. E. et al. Transcapillary fluid shifts in tissues of the head and neck during and after simulated microgravity. *J. Appl. Physiol.* **71**, 2469–2475 (1991).
8. Ong, J., Mader, T. H., Gibson, C. R., Mason, S. S. & Lee, A. G. Spaceflight associated neuro-ocular syndrome (SANS): an update on potential microgravity-based pathophysiology and mitigation development. *Eye (Lond.)* **37**, 2409–2415 (2023).
9. Zwart, S. R. et al. Association of genetics and B Vitamin status with the magnitude of optic disc edema during 30-day strict head-down tilt bed rest. *JAMA Ophthalmol.* **137**, 1195–1200 (2019).
10. Andreev-Andrievskiy, A. et al. Mice in Bion-M 1 space mission: training and selection. *PLoS. One* **9**, e104830 (2014).
11. Hargens, A. R., Steskal, J., Johansson, C. & Tipton, C. M. Tissue fluid shift, forelimb loading, and tail tension in tail-suspended rats. *Physiologist* **27**, S37–S38 (1984).
12. Grove, D. S., Pishak, S. A. & Mastro, A. M. The effect of a 10-day spaceflight on the function, phenotype, and adhesion molecule

expression of splenocytes and lymph node lymphocytes. *Exp. Cell Res.* **219**, 102–109 (1995).
13. Gaignier, F. et al. Three weeks of murine hindlimb unloading induces shifts from B to T and from th to tc splenic lymphocytes in absence of stress and differentially reduces cell-specific mitogenic responses. *PLoS One* **9**, e92664 (2014).
14. Chapes, S. K., Mastro, A. M., Sonnenfeld, G. & Berry, W. D. Antiorthostatic suspension as a model for the effects of spaceflight on the immune system. *J. Leukoc. Biol.* **54**, 227–235 (1993).
15. Aviles, H., Belay, T., Fountain, K., Vance, M. & Sonnenfeld, G. Increased susceptibility to Pseudomonas aeruginosa infection under hindlimb-unloading conditions. *J. Appl. Physiol.* **95**, 73–80 (2003).
16. Moore, T. P. & Thornton, W. E. Space shuttle inflight and postflight fluid shifts measured by leg volume changes. *Aviat. Space Environ. Med.* **58**, A91–A96 (1987).
17. Lurie, F. et al. The American Venous Forum, American Vein and Lymphatic Society and the Society for Vascular Medicine expert opinion consensus on lymphedema diagnosis and treatment. *Phlebology* **37**, 252–256 (2022).
18. Executive Committee of the International Society of Lymphology. The diagnosis and treatment of peripheral lymphedema: 2020 Consensus Document of the International Society of Lymphology. *Lymphology* **53**, 3–19 (2020).
19. Lin, Y. et al. Manual lymphatic drainage for breast cancer-related lymphedema: a systematic review and meta-analysis of randomized controlled trials. *Clin. Breast Cancer* **22**, e664–e673 (2022).
20. Arends, C. R., van der Molen, L., van den Brekel, M. W. M. & Stuiver, M. M. Test-retest reliability of a protocol for assessment of local tissue water in the head and neck area. *Lymphat. Res. Biol.* **22**, 12–19 (2024).
21. Kiely, M. J., Poulsen, A., Muschamp, S. D., Sallis, C. & Whiteley, M. S. Participant reported improvement in cellulite by Vari-Pad apparel and objective measurements - a "first use" pilot study. *Clin. Cosmet. Investig. Dermatol.* **16**, 2573–2583 (2023).
22. Mekari, S. et al. The impact of a short-period head-down tilt on executive function in younger adults. *Sci. Rep.* **12**, 20888 (2022).
23. Andersen, C., Reiter, H. J. & Marmolejo, V. L. Redefining wound healing using near-infrared spectroscopy. *Adv. Skin Wound Care* **37**, 243–247 (2024).
24. Myllyla, T. et al. Assessment of the dynamics of human glymphatic system by near infrared spectroscopy. *J. Biophotonics* **11**, e201700123 (2018).
25. Kawai, Y. et al. Cerebral blood flow velocity in humans exposed to 24 h of head-down tilt. *J. Appl. Physiol.* **74**, 3046–3051 (1993).
26. Kurihara, K., Kikukawa, A. & Kobayashi, A. Cerebral oxygenation monitor during head-up and -down tilt using near-infrared spatially resolved spectroscopy. *Clin. Physiol. Funct. Imaging* **23**, 177–181 (2003).
27. Schneider, S. et al. Changes in cerebral oxygenation during parabolic flight. *Eur. J. Appl. Physiol.* **113**, 1617–1623 (2013).
28. Langemo, D. K. & Spahn, J. G. A reliability study using a long-wave infrared thermography device to identify relative tissue temperature variations of the body surface and underlying tissue. *Adv. Skin Wound Care.* **30**, 109–119 (2017).
29. Chanmugam, A. et al. Relative temperature maximum in wound infection and inflammation as compared with a control subject using long-wave infrared thermography. *Adv. Skin Wound Care* **30**, 406–414 (2017).
30. Holster, M. Driving outcomes and improving documentation with long-wave infrared thermography in a long-term acute care hospital. *Adv. Skin Wound Care* **36**, 189–193 (2023).
31. Pandiarajan, M. & Hargens, A. R. Ground-based analogs for spaceflight. *Front. Physiol.* **11**, 716 (2020).
32. Watenpaugh, D. E. Analogs of microgravity: head-down tilt and water immersion. *J. Appl. Physiol.* **120**, 904–914 (2016).
33. Cromwell, R. et al. Overview of the NASA 70-day bed rest study. *Med. Sci. Sports Exerc.* **50**, 1909–1919 (2008).
34. Solari, E., Marcozzi, C., Negrini, D. & Moriondo, A. Lymphatic vessels and their surroundings: how local physical factors affect lymph flow. *Biology (Basel)* **9**, 463 (2020).
35. Solari, E. et al. TRPV4 channels' dominant role in the temperature modulation of intrinsic contractility and lymph flow of rat diaphragmatic lymphatics. *Am. J. Physiol. Heart Circ. Physiol.* **319**, H507–H518 (2020).
36. Crisóstomo, R. S., Candeias, M. S. & Armada-da-Silva, P. /A. Venous flow during manual lymphatic drainage applied to different regions of the lower extremity in people with and without chronic venous insufficiency: a cross-sectional study. *Physiotherapy* **103**, 81–89 (2017).
37. Dos Santos Crisóstomo, R. S., Candeias, M. S., Ribeiro, A. M., da Luz Belo Martins, C. & Armada-da-Silva, P. A. Manual lymphatic drainage in chronic venous disease: a duplex ultrasound study. *Phlebology* **29**, 667–676 (2014).
38. Breslin, J. W. et al. Lymphatic vessel network structure and physiology. *Compr. Physiol.* **9**, 207–299 (2019).
39. Freeborn, T. J., Critcher, S. & Hooper, G. Segmental tissue resistance of healthy young adults during four hours of 6-degree head-down-tilt positioning. *Sensors (Basel)* **23**, 2793 (2023).
40. Freeborn, T. J., Critcher, S. & Hooper, G. L. Short-term segmental bioimpedance alterations during 6° head-down tilt. *Annu. Int. Conf. IEEE Eng. Med. Biol. Soc.* **2021**, 6974–6977 (2021).
41. Whittle, R. & Diaz-Artiles, A. Gravitational effects on carotid and jugular characteristics in graded head-up and head-down tilt. *J. Appl. Physiol.* **134**, 217–229 (2023).
42. Marshall-Goebel, K. et al. Assessment of jugular venous blood flow stasis and thrombosis during spaceflight. *JAMA Netw. Open.* **2**, e1915011 (2019).
43. Bhave, G. & Neilson, E. G. Body fluid dynamics: back to the future. *J. Am. Soc. Nephrol.* **22**, 2166–2181 (2011).
44. Reybrouck, T. & Fagard, R. Gender differences in the oxygen transport system during maximal exercise in hypertensive subjects. *Chest* **115**, 788–792 (1999).
45. Sevick-Muraca, E. M., Fife, C. E. & Rasmussen, J. C. Imaging peripheral lymphatic dysfunction in chronic conditions. *Front. Physiol.* **14**, 1132097 (2022).
46. Rasmussen, J. C. et al. Assessing lymphatic route of CSF outflow and peripheral lymphatic contractile activity during head-down tilt using near-infrared fluorescence imaging. *Physiol. Rep.* **8**, e14375 (2020).
47. Dávalos, M. P. A., Brioschi, M. L., da Rosa, S. E., Brioschi, G. C. & Neves, E. B. Can dual infrared-visual thermography provide a more reliable diagnosis of perforator veins and reflux severity? *J. Clin. Med.* **12**, 7085 (2023).
48. Uren, R. F., Howman-Giles, R. & Thompson, J. F. Patterns of lymphatic drainage from the skin in patients with melanoma. *J. Nucl. Med.* **44**, 570–582 (2003).
49. Uematsu, S., Edwin, D. H., Jankel, W. R., Kozikowski, J. & Trattner, M. Quantification of thermal asymmetry. Part 1: normal values and reproducibility. *J. Neurosurg.* **69**, 552–555 (1988).
50. Maier, M. & Lakens, D. Justify your alpha: a primer on two practical approaches. *Adv. Meth. Pract. Psychol. Sci*. **5**, https://doi.org/10.1177/25152459221080396 (2022).

Acknowledgements

The authors would like to thank Drs. Alan R. Hargens (University of California, San Diego, La Jolla, CA), Melissa B. Aldrich (The University of Texas, Health Science Center at Houston, Houston, TX), John Rasmussen (The University of Texas, Health Science Center at Houston) and Joshua Ong (University of Michigan, Kellogg Eye Center, Ann Arbor, MI) for their review of the manuscript prior to submission. The authors would also like to thank Kent

Imaging, WoundVision, and Delfin Technologies for their in-kind donations of the equipment used during the study. This study was funded by Nova Southeastern University. The funder played no role in the study design, data collection, analysis, and interpretation of data, or the writing of this manuscript.

Author contributions

H.B.: study design, implementation, data collection, data analysis, and writing of the manuscript; F.A.: study design, implementation, data collection, and data analysis; J.P., N.S., C.H.: implementation, data collection; P.H. and K.A.E.: study design, data analysis, and writing of the manuscript; S.G.: study design, data collection, and implementation; H.M.: study design; M.M.M.: study design, data analysis, and writing of manuscript. All authors reviewed and approved the final manuscript.

Competing interests

Aviles is KOL for WoundVision. Eckert was a paid consultant for Strategic Solutions, which received funding from NSU for its work in this study. The remaining authors declare no competing interests.

Additional information

Correspondence and requests for materials should be addressed to M. Mark Melin.

Reprints and permissions information is available at http://www.nature.com/reprints

Publisher's note Springer Nature remains neutral with regard to jurisdictional claims in published maps and institutional affiliations.

Open Access This article is licensed under a Creative Commons Attribution-NonCommercial-NoDerivatives 4.0 International License, which permits any non-commercial use, sharing, distribution and reproduction in any medium or format, as long as you give appropriate credit to the original author(s) and the source, provide a link to the Creative Commons licence, and indicate if you modified the licensed material. You do not have permission under this licence to share adapted material derived from this article or parts of it. The images or other third party material in this article are included in the article's Creative Commons licence, unless indicated otherwise in a credit line to the material. If material is not included in the article's Creative Commons licence and your intended use is not permitted by statutory regulation or exceeds the permitted use, you will need to obtain permission directly from the copyright holder. To view a copy of this licence, visit http://creativecommons.org/licenses/by-nc-nd/4.0/.

© The Author(s) 2024